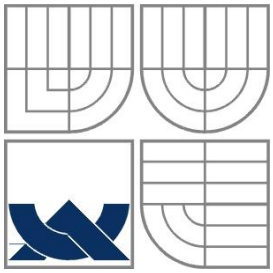

VYSOKÉ UČENÍ TECHNICKÉ V BRNĚ
BRNO UNIVERSITY OF TECHNOLOGY

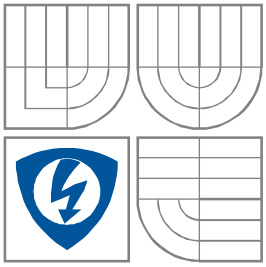

FAKULTA ELEKTROTECHNIKY A KOMUNIKAČNÍCH TECHNOLOGIÍ
ÚSTAV BIOMEDICÍNSKÉHO INŽENÝRSTVÍ

FACULTY OF ELECTRICAL ENGINEERING AND COMMUNICATION
DEPARTMENT BIOMEDICAL ENGINEERING

ODSTRAŇOVAČ ZUBNÍHO KAMENE

ELIMINATOR OF DENTAL CALCULUS

DIPLOMOVÁ PRÁCE
MASTERS'S THESIS

AUTOR PRÁCE — Bc. ROSTISLAV HALAŠ
AUTHOR

VEDOUCÍ PRÁCE — doc. Ing. JIŘÍ ROZMAN, CSc.
SUPERVISOR

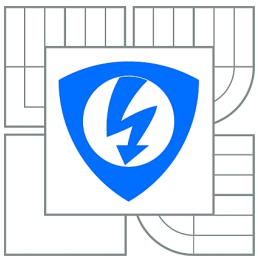

VYSOKÉ UČENÍ TECHNICKÉ V BRNĚ

Fakulta elektrotechniky a komunikačních technologií

Ústav biomedicínského inženýrství

Diplomová práce

magisterský navazující studijní obor
Biomedicínské a ekologické inženýrství

Student:	Bc. Rostislav Halaš	***ID:***	73034
Ročník:	2	***Akademický rok:***	2010/2011

NÁZEV TÉMATU:

Odstraňovač zubního kamene

POKYNY PRO VYPRACOVÁNÍ:

Seznamte se s ultrazvukovou metodou odstraňování zubního kamene. Pro vypracovaný systémový návrh takového zařízení navrhněte obvodové řešení. Nástroj má využívat vrstvenný ultrazvukový měnič pracující na frekvenci 27 kHz s intenzitou ultrazvuku do 5 W/cm2. Napájení ze sítě.
Práce musí obsahovat : teoretický rozbor, schéma zapojení, soupisku součástek a výkres plošného spoje.

DOPORUČENÁ LITERATURA:

[1] ROZMAN J.: Ultrazvuková technika v lékařství. VUT FE, Brno, 1979
[2] PUNČOCHÁŘ J.: Operační zesilovače. BEN, Praha, 1996

Termín zadání:	15.10.2010	***Termín odevzdání:***	20.5.2011

Vedoucí práce: doc. Ing. Jiří Rozman, CSc.

prof. Ing. Ivo Provazník, Ph.D.
Předseda oborové rady

UPOZORNĚNÍ:

Abstrakt

Tato práce se zabývá návrhem ultrazvukového odstraňovače zubního kamene pracujícím na frekvenci 27 kHz s maximální intenzitou ultrazvuku 5W/cm^2. Popisuje mechanismus vzniku zubního kamene, důsledky na zdraví a metody jeho odstraňování. Zaměřuje se na principy odstraňování s využitím ultrazvukového vlnění. Dále je sestaveno funkční a blokové schéma. Na základě těchto znalostí je proveden návrh a výpočet jednotlivých částí aplikátoru. Výkonové a napěťové poměry jsou vypočítány od aplikačního hrotu směrem ke generátoru. V neposlední řadě je popsán návrh obvodů buzení měniče i kontrolních obvodů. Schémata jsou doplněna výkresy desek plošných spojů a soupiskou součástek.

Abstract

This project is focused on the design of the ultrasonic dental scaler with the working frequency 27 kHz and the maximal ultrasound intensity 5W/cm^2. It describes the process of the calculus creation, its effect on health and methods of removal. Especially, the ultrasonic method of removal is deeply discussed. Furthermore, the functional and block diagrams are built. On the basis of this knowledge, the design and calculation of the applicator part is carried out. The power and voltage values are calculated from the tip towards the generator output. Last but not least, the design of the circuits of the transducer supply and control part is described. The diagrams are supplemented by the drawings of the printed circuit boards and part lists.

Klíčová slova

Zubní kámen, odstraňování, vrstvenný měnič, ultrazvuk, vlnovod, generator, řídící obvody, zdroj.

Keywords

Dental calculus, removal, ultrasound, sandwich transducer, sonotrode, generator, control circuits, power supply.

Bibliografická citace: HALAŠ, R. *Eliminator of dental calculus: diplomová práce.* Brno: FEKT VUT v Brně, 2011. 71 s., 2 příl.

Prohlášení

Prohlašuji, že svou diplomovou práci na téma Eliminator of dental calculus jsem vypracoval samostatně pod vedením vedoucího diplomové práce a s použitím odborné literatury a dalších informačních zdrojů, které jsou všechny citovány v práci a uvedeny v seznamu literatury na konci práce.

Jako autor uvedené diplomové práce dále prohlašuji, že v souvislosti s vytvořením této diplomové práce jsem neporušil autorská práva třetích osob, zejména jsem nezasáhl nedovoleným způsobem do cizích autorských práv osobnostních a jsem si plně vědom následků porušení ustanovení § 11 a následujících autorského zákona č. 121/2000 Sb., včetně možných trestněprávních důsledků vyplývajících z ustanovení § 152 trestního zákona č. 140/1961 Sb.

V Brně dne 30. června 2011 .....
podpis autora

Poděkování

Děkuji vedoucímu diplomové práce doc. Ing. Jiřímu Rozmanovi, CSc. za účinnou metodickou, pedagogickou a odbornou pomoc a další cenné rady při zpracování mé diplomové práce.

V Brně dne 30. června 2011 .....
podpis autora

Content

1. Introduction

Design of medical devices belongs to the most dynamically developing branches of electro technical industry. Especially, in recent twenty years there has been a significant “boom” of electronic medical devices in association with expansion of miniaturized electronics.

Newly designed devices measurably speed up classical treatment and enable use of new diagnostics or therapy procedures. Last but not least there is an effort to make the treatment for both doctor and patient as comfortable as possible.

In this sense stomatology is a very specific part of healthcare. There are some electronic devices used with every treatment. These devices are usually built into a dentist chair. Also dental scaler is very important part of the dentist office equipment. The reason is that dental scaler, sometimes called tartar, is one of the most common causes of teeth illnesses. Unfortunately it cannot be easily removed at home and then it is the right time for professional treatment. Formerly, the dental calculus used to be removed mechanically; however this method was rough, time consuming, and sometimes painful for the patient. Nowadays, the ultrasound technique is used with advance.

The aims of this work are to describe the mechanism of the dental calculus creation and also possible methods of its removal. It should focus mainly on the ultrasonic method of the dental calculus removal.

However, the main part of this thesis should consist of the design of the scaler device using the ultrasonic sandwich transducer. The assigned working frequency of the transducer is 27 kHz. The maximal intensity of the ultrasound at the tip is 5 W/cm^2. The device is supposed to use an electric network supply.

The design will be described step-by- step, so that the reader would be able to easily follow the procedure. The thesis will also include connection diagram, part-lists and printed circuit board layouts, so that the device would be ready to build

Fig. 1.1 Dental scale removal

2. Dental calculus origin and its removal

2.1 Dental calculus

Dental calculus is a phenomenon affecting the major part of worldwide population. Together with gingivitis, it is recognized as the most frequent teeth disease. There are two types of calculus [1]:

- Supra-gingival – rises on the surface of teeth and gingivae
- Sub-gingival– formed in the crevice between the tooth cervix and the gingiva

Dental calculus (also called tartar) is as a matter of fact calcified dental plaque that consists mainly of mineral salts of calcium laid between the residual parts of microorganisms.

Fig. 2.1 Dental scale

It is perfectly normal that our mouths are full of microorganisms. However, after a longer time of bad oral hygiene or wrong cleaning technique, the microorganisms are settling down on the teeth surface and creating, together with ions brought by salivary glands, a thin biofilm. This thin film is called plaque. Later, the dental plaque stored in many layers starts calcifying. It solidifies and creates a compact crust on the tooth surface. The crust has yellow-white (in the case of smoker yellow-brown) color. The thickest part is usually close about dental cervices.

Supra-gingival calculus is unsightly; its color is influenced by pigment contained in food, beverages and tobacco. Furthermore, its rough surface enables settling of life microorganisms that can cause gingivitis or caries. Last but not least, it can exasperate the outer side of gingivae [2].

Sub-gingival calculus exposes the dental cervicae to the environment of buccal cavity. This effect contributes to the rise of parodontitis (bacterial infection of supplement tooth tissues). It begins with gingivae bleeding, later the parodontitic pockets are created, gingivae recede and the positioning of teeth is changing (spacing, deviation). As a consequence, the teeth are released from gingivae.

The amount of dental calculus is population dependant. It is influenced by hygienic habits, professional care access, food composition, age, medicament usage, etc. [1].

In populations that combine periodic oral hygiene and occasional professional treatment the supra-gingival calculus is usually located on surfaces surrounding salivary glands. Once the layer of plaque gets hard, it is no more removable by toothbrush. Therefore it is necessary to undergo professional treatment.

It should be obvious, from all of the above mentioned facts, that regular dental calculus removal is an important part of dental care. The main techniques for dental tartar removal will be described in the following chapter.

2.2 Commonly used techniques for dental calculus removal

According to [1], the three commonly used techniques are based on utilization of mechanical, pneumatic and ultrasonic energy. However, the most popular technique is ultrasonic scaling. The brief description of mentioned methods follows:

A) Mechanical – special tools such as scalers (one sided tool), kyrets (both sided tool), scratch tools, etc. Fig. 2.2 [5] shows some of these tools. They usually consist of handle, sleeve and tip. It is the oldest method; it has been used for hundreds of years. Every dentist is trained how to use this method. In comparison with other methods, the tools are cheaper and lighter. Therefore the treatment can be more exact. Despite the fact that it is often mentioned as old-fashioned and more painful method, it still remains suitable for removal of subgingival dental calculus, where accuracy and delicacy is necessary.

The main disadvantage is duration of the treatment. It is demanding for both dentist and patient. Furthermore it is more painful than the ultrasonic method.

Fig. 2.2 Dental scale removal tools

B) Ultrasonic – this method is based on the effect called cavitation. The high energy ultrasonic field generates small "bubbles" called cavities. These cavities collapse in a short time and release a large amount of mechanical energy that can cause a damage of dental scale structures. Nowadays, it is the most commonly used method. Patients feel lower pressure on their teeth; the treatment is therefore more comfortable, less painful and shorter in duration. The device is also very silent. None disadvantages are worth to mention, except higher price of the apparatus. During last few years, the ultrasonic scaler has become the common part of dentist equipment. This very important method will be deeply discussed in next chapters.

C) Pneumatic – this method has not been used very often. Despite, it is mentioned to allow the reader to compare other ways of calculus removal. In principle, the asymmetric air-driven rotor generates vibrations that are transmitted towards the tip. A massive cooling must be provided to avoid overheating of the tip. The apparatus is cheaper, than ultrasonic scaler; however there are more disadvantages to consider, such as high irregular vibrations of the tip that can cause extensive roughness of treated surfaces.

2.3 Ultrasound and its application in dental calculus removal

Ultrasound waves are a form of mechanical waves in solid, fluid or gas environment. The frequency of these waves lies between 16 kHz and 1 GHz.

The definition of wave motion is propagation of mechanical energy via chemical bonds in a physical environment. The oscillations of particles are transmitted to other particles in the direction of propagation. The speed of ultrasonic waves depends on physical aspects of the environment [3].

There are two types of waves-transversal and longitudinal. In a liquid and gaseous environment only longitudinal oscillations arise. They oscillations axis of longitudinal waves is in the same direction as the direction of wave propagation. Longitudinal wave exhibit periodical changing of particles density in the direction of propagation.

In solids, the transversal waves can also occur. In this case the oscillations axis is oriented perpendicular to the propagation direction. There is no change in both pressure and particles density [3].

The velocity of ultrasonic wave propagation $\left[\frac{\mathrm{m}}{\mathrm{s}}\right]$ can be computed as [3]:

$$v = \sqrt{\frac{K}{\rho}}\,, \tag{2.1}$$

where *K [MPa]* is the modulus of elasticity of the medium and ρ [kg/m^3] is the density of the medium, which the ultrasonic waves propagate in.

Another physical quantity is related to velocity of wave propagation and density of the environment, it is called acoustic impedance $Z\,[Pa \cdot s \cdot m^{-1}]$. It can be expressed by the equation [3]:

$$Z = \rho \cdot v\,. \tag{2.2}$$

The energy of ultrasonic waves can be quantitatively expressed by the physical quantity called intensity of ultrasound $\left[\frac{W}{m^2}\right]$, which is formulated as [4]:

$$I = \frac{dW}{dS} \cdot \frac{1}{t}, \tag{2.3}$$

where *dW* is power that perform perpendicular towards the plane *dS* in a unit of time *t*.

Then for a harmonic signal can be used the formula [3]:

$$I = \frac{p^2}{2 \cdot \rho \cdot v}\,, \tag{2.4}$$

where *p* is magnitude of the acoustic pressure caused by ultrasonic waves.

Some effects accompany the propagation of ultrasonic waves in a medium:

- Attenuation of the ultrasonic energy – a part of the energy of waves is absorbed by the medium, it can be described by the formula [4]:

$$I_x = I_0 \cdot e^{-2 \cdot \alpha \cdot x}\,, \tag{2.5}$$

where I_x is the intensity of ultrasound in the distance *x* from a source of waves. I_0 is the original intensity produced by a source of ultrasonic waves and α is the attenuation coefficient specific for each medium. It is necessary to mention that the attenuation coefficient is frequency dependent. For materials which are used for ultrasonic devices construction (titanium, steel, etc.) the attenuation coefficient is so small that can be neglected.

- Reflection – this effect appears on the boundary of two mediums with different acoustic impedance. It is described by the reflection coefficient [-], that can be computed using formula [4]:

$$r = \frac{I_r}{I_i} = \left(\frac{Z_2 - Z_1}{Z_2 + Z_1}\right)^2, \tag{2.6}$$

I_r implies the reflected wave intensity, I_i the incident wave intensity, Z_2 and Z_1 are the values of acoustic impedance in each medium.

The generators of ultrasonic waves are called transducers. They convert one kind of energy, such as electric, mechanical, etc., into the energy of mechanical waves in the frequency range of ultrasonic waves. We can imagine a generator as an oscillating plate that periodically compresses the surrounding medium. These pressure variations further propagate by the mechanism which was described earlier

In medical use, the effect of ultrasound on human body must be assessed. These effects can be divided into the following categories [1]:

- Mechanical – micro-vibration and cavitation effect occur. The micro-vibration usually cause micro-massage of tissues and increase the speed of cell metabolism. The cavitation effect is much stronger. Details will be discussed later.

- Thermal – the mechanical energy absorbed in tissues is converted into heat. This may cause overheating of tissues and cell death.

- Chemical – ultrasonic waves increase the speed of chemical processes and their course.

From all of the above mentioned effects cavitation is the main phenomenon used in ultrasonic dental scaling. That effect is caused by nonlinear oscillations of fluid medium particles. It is based on creation of cavities in the places where local pressure decrease is present. At the beginning the cavity is filled by vacuum, later some gases from surrounding area may diffuse into the inner space of cavity "bubble". As the pressure increases, the cavity collapses and creates a shock wave that has destructive effect on the ambient matter [3].

The mechanism of ultrasonic calculus removal is therefore based on cavities occurrence. The working tip is oscillating with the frequency in the range of ultrasonic waves. After water is injected on the working tip, the energy of oscillations causes creation of cavity "bubbles". In a very short time they concentrate a lot of energy and implode. Those cavities they got into the slot located between and enamel produce above mentioned shock wave that is able to erode the surface of dental calculus and the layer of calculus fell apart. The flow of water drains the debris out of the tooth surface [3].

3. System design

In this chapter the design of the ultrasonic dental scaler is described step by step. First, the functional diagram is built up. Then the block diagram of whole device is mentioned followed by more detailed description of design of the single blocks of applicator. In the last part, the voltage and power values are computed from the tip of applicator to the transducer excitation (e.g. generator). During whole text the cross-influence of the single parts and feasibility of construction are discussed.

3.1 Functional diagram

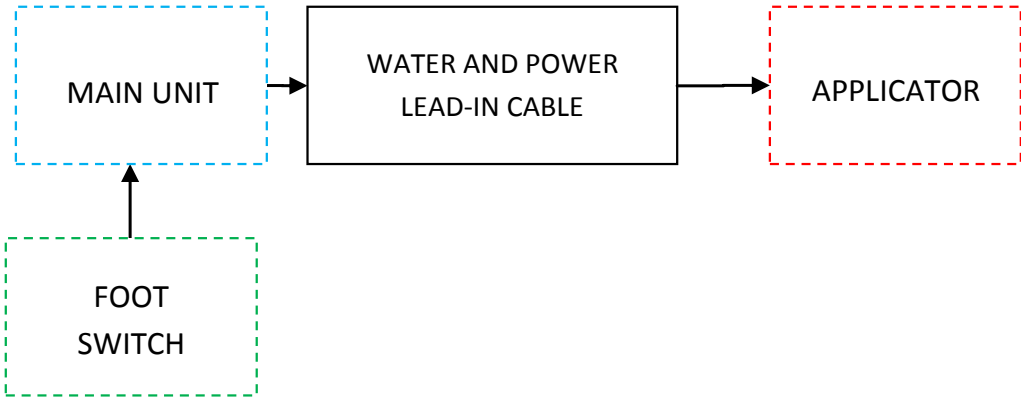

Fig. 3.1 Functional diagram

Functional diagram (Fig. 3.1.) consists of four parts. Those are main supply and control unit, lead-in cable, applicator and foot switch. The main unit construction can be designed as [5]:

1) Modular – the module of this unit can be easily connected with currently used dental chair. The advantage of this version is in the fact, that it can use all the leads built in to dental chair, therefore there is no need to do any additional construction work before use. However a problem may occur if there is a requirement to design a device compatible with products of various manufacturers. In this case there are some limiting features such as dimensions and interface, communication, etc.

2) Table-type – the device can be used independently on any other equipment. The design must include own power supply, control circuits and water inlet. On the other hand, it can be moved according to current needs (limiting factor is only the length of leads). In this case the dimensions of whole device are not crucial, however it is necessary to design case including display, buttons, shape of case, etc. Nowadays it is

not only quality and price, but also exterior of a device which is important for consumers.

3) Mobile – this variant is also independent on any other equipment. In addition to the table-type it has its own water tank. As a power supply batteries are used, so there is no need for any cable leads. The advantage is portability and compactness. However the operational time is limited by capacity of batteries and the amount of water. In fact the volume of water reservoir (usually 500ml [6]) is not so limiting, as the consumption of water for a treatment of one patient is about 20ml [6]. The volume of reservoir is therefore sufficient for whole day treatment.

Another block of the functional diagram is lead-in cable. It contains electric wires connecting the main unit and the applicator part. It also includes a water tube that links valve in the main unit and rigid tube mounted inside the applicator. The cable must be mechanically robust with isolation adequate to work environment. As the wave length of signal is quite high in comparing with length of cable (typically 2-3m), there is no need to match the impedance of the cable to the driving circuits and transducer.

The applicator is round shaped with ergonomic grip surface. At the distant part of applicator is mounted a work tip (Fig. 3.2), which is inserted to the oral cavity. There are various types of tips with different dimensions, angles, applications. They are usually made of stainless steel or titanium. Those materials have good characteristic for ultrasound propagation and products can be easily sanitize (e.g. in autoclave at temperatures about 130°C).

The last part is foot switch. This switch allows to a dentist to switch on/off the device, resp. control the intensity of ultrasound and amount of water applied on the tip. This unusual way of control is typical for medical devices, especially for devices used by dentists. Using foot-switch allows a dentist to fully focus on treatment without need to use lay down the applicator and adjust the power by hand.

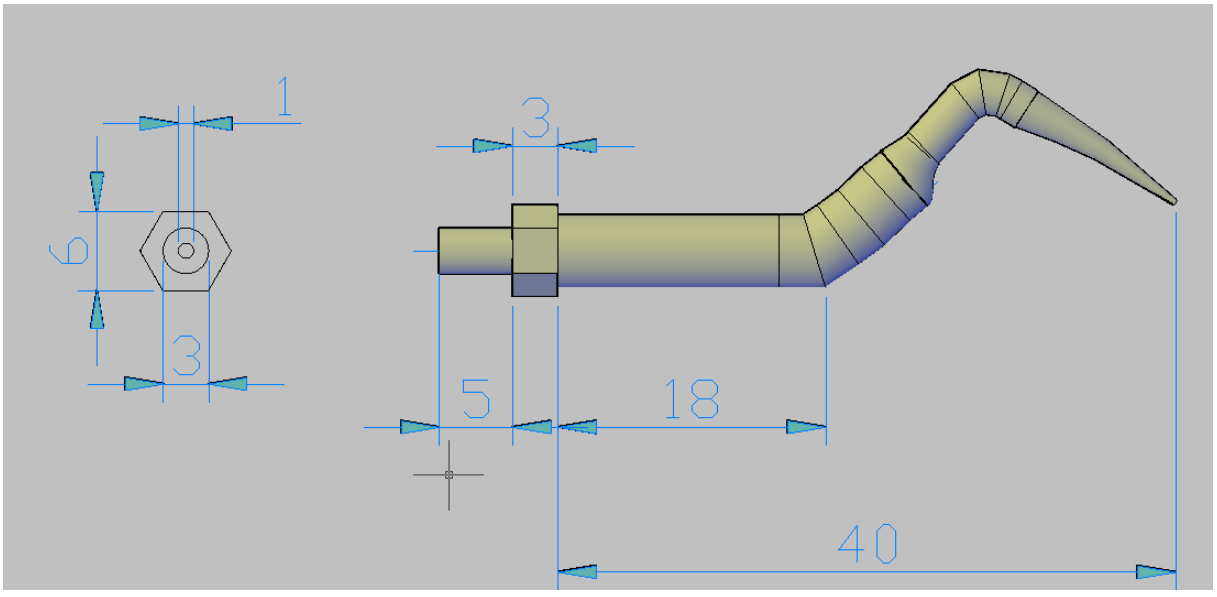

Fig. 3.2 Work tip Amdent 37R

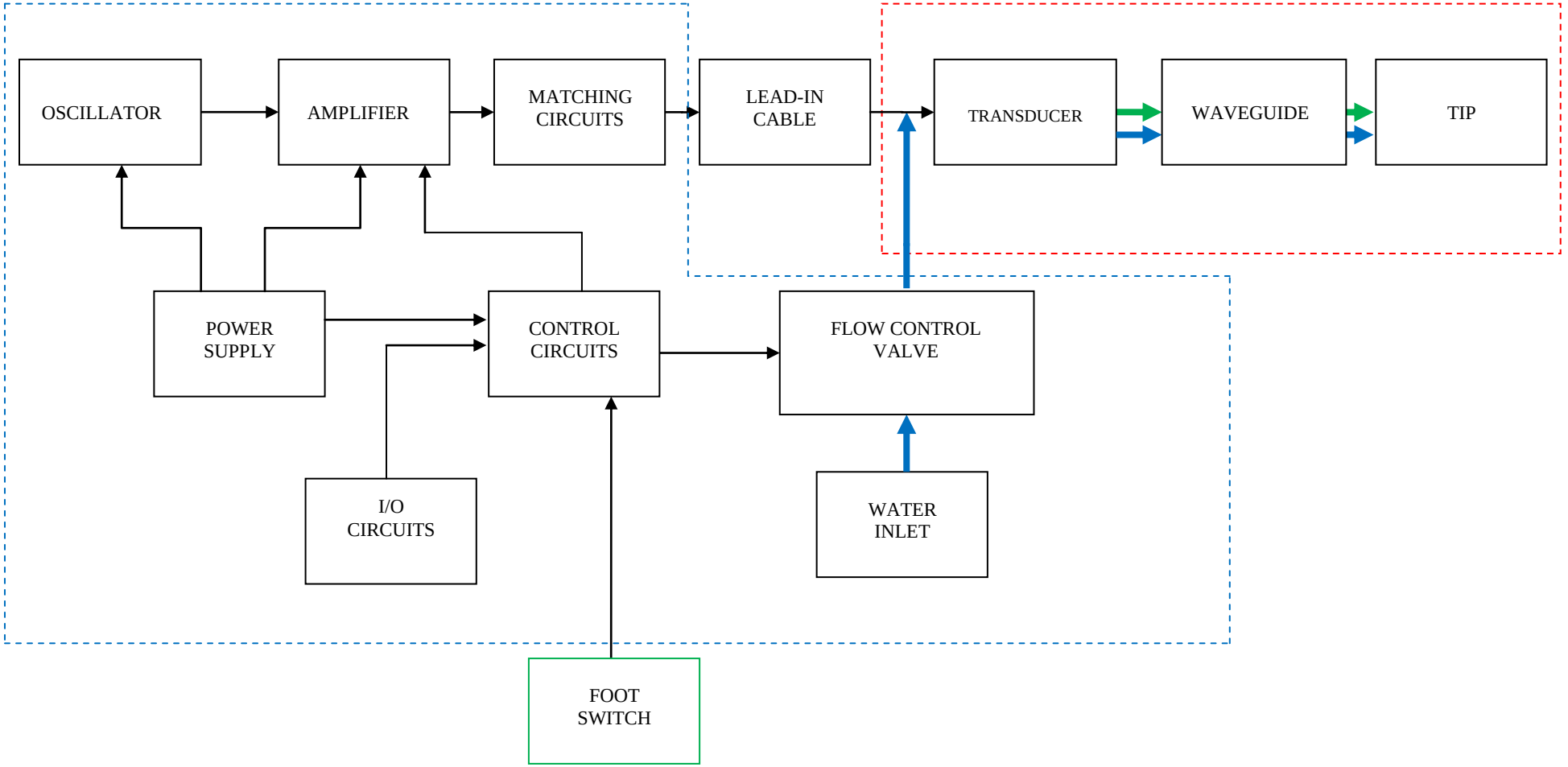

Fig. 3.3 Block diagram of the ultrasonic dental scaler

3.2 Block diagram

In the previous chapter, the account of functional diagram structure was given. The structure of the device is more depicted more detailed on Fig. 3.3, which is a block diagram of ultrasonic dental scaler. Main parts from functional diagram (Fig. 3.1.) are framed by dashed line. Less detailed block diagrams can be found for example in [3] or [10].

The main line consists of oscillator, which generates basic harmonic signal on a frequency equal to work frequency of the transducer. Optionally, the harmonic signal shape can be change by shaping circuits (e.g. rectangular impulses). Further, there is a tuned amplifier (one-, bi- or more-stage according to driving power). Tuned oscillator is used in order to amplify only useful part of signal and attenuate the adverse components of signal generated by oscillator. As the input impedance of the transducer and the output impedance of the oscillator vary, there must be a matching circuit inserted between these two parts. The matching circuit provides the optimal energy transfer towards the transducer.

Next block of control unit is used for propagation of water flow towards the working tip. It contains water inlet, which is connected to an outlet in a dental office or a dental chair. It is followed by a valve that controls the amount of water flowing in the tube and the pipe inside the applicator.

Another important block is called control circuits. These circuits can be analogue or digital (with use of a microprocessor). This block is used to control the level of ultrasound intensity at work tool, the water valve (amount of water) and temperature of the device. It also ensures the protection against overheating, low power supply voltage, other errors. There is also an interface used for communication with user (I/O circuits block). It comprises of some I/O devices such as a keyboard, a display, monitoring LED diodes, etc. Furthermore, there can be a communication interface (e.g. RS232, USB) which allows communication with other devices, change of firmware, etc. Power supply unit is used to convert mains supply voltage (alternating, 230V) into direct voltage suitable to supply devices included in all the circuits. The main supply must be electrically isolated from the other circuits to prevent interaction of the main supply voltage with a patient.

Blocks of foot switch and lead-in cable has already been discussed. So another functional group can be described. It is framed by red dashed line. It contains the sandwich transducer that converts electrical energy into mechanical energy. At the end of transducer structure a waveguide is attached. The waveguide has two functions. It allows changing the cross-section of tip into size suitable for treatment and mounting of work tip. It also works as ultrasonic wave amplifier. The intensity of ultrasound is few times higher at the end than at the beginning. The amplification coefficient depends on shape of waveguide and will be discussed later.

Last but not least part is work tip. That is the part that is inserted into patient’s mouth. There are various shapes depending mainly on the kind of treatment. According to [6], nowadays, there are only a few big companies that manufacture work tips.

One of the leading companies on the European market is the Swedish company Amdent AB, owned by the concern LM Instruments. Shapes and bonds are standardized, so it is possible to use them in all of the concern devices. The scaling tips are made of titanium.

3.3 Piezoelectric transducers

3.3.1 Basic facts

The piezoelectric effect was discovered in 1880 by Pierre Curie [9]. This effect is specific for some crystallic materials, such as silicium or tourmaline crystals. Since 50's of the twentieth century, some artificial materials have been developed, such as barium-titanate (PBT) or lead-zirconium-titanate (PZT). These materials (ceramics) have much better physical and chemical properties than natural crystals. Properties of artificial materials can be easily modified and the reproducibility is on a high level.

The basic idea of piezoelectric effect is that, if a mechanical pressure is applied on a crystal, the electric voltage appears between two opposite sides of crystal. A reverse piezoelectric effect can be defined as changes in dimensions of crystal caused by applied electric field.

The deformation behavior depends on location of electrodes and electric field orientation. If an alternating electric field is applied, the structure shrinks and stretches periodically. So in a material environment, such structure becomes a source of mechanical waves that can propagate further to space.

However, above described mechanism is significantly simplified. In the real world, the value of magnitude of such oscillations is in the order micrometers. Real crystals are anisotropic. This means that electrical, mechanical and electromechanical properties are related to direction of applied forces.

In order to determinate properties in the right direction, a crystallographic system of three orthogonal axes is used [9]. In most of publications theses axes are assigned to numbers 1, 2, and 3 that are corresponding to the x, y, and z signs of the Cartesian coordinate system.

Artificial piezoelectric materials are usually isotropic in its original state, however once they are polarized, they become also anisotropic. The actuating field is usually applied in the plane perpendicular to axis 3(also signed as 3). In this plane and in all of the coplanar planes, the crystal has anisotropic properties [11].

3.3.2 Dynamic properties of the piezoelectric transducer

Once the electrodes are bonded to the piezoelectric crystal made of synthetic ceramics, we get the basic piezoelectric transducer. In following text, only this configuration is stated as transducer, natural crystals are no more considered.

For examination of dynamical behavior of a piezoelectric transducer, a substitution diagram can be used [3], see Fig. 3.4. A crystal between two electrodes can be modeled as a capacitor with capacity C0 and dielectric losses expressed by the resistor RD. The second line of substitution diagram simulates the oscillating properties

of the crystal and determines the natural frequency of oscillations. If the frequency of oscillations corresponds to its natural frequency, then the resistance of the transducer is equal to value of resistance RM.

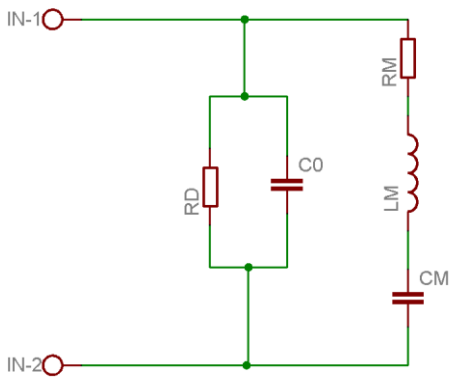

Fig. 3.4 Substitution diagram of a piezoelectric transducer

A typical example of pattern of the module of the electric impedance of a transducer can be seen on Fig. 3.5 [11]. There are two significant peaks in the pattern. – f_m equal to resonance and f_n equal to anti-resonance frequency. In most of the cases, the resonant frequency is used for ultrasonic devices. Then, the anti-resonance frequency is required to be as far as possible from the resonance frequency. If they are too close the frequency of oscillations can alternate between these two values [12].

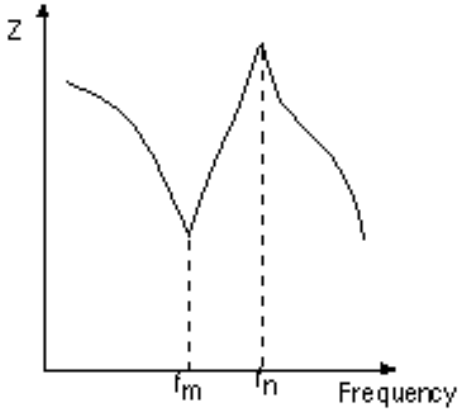

Fig. 3.5Module impedance characteristic of a piezoelectric transducer

The static capacity C0 can cause some problems. When the transducer is driven by alternating source that capacity is being periodically charged and uncharged and therefore it uses some extra current from generator. To neutralize the capacity, a coil in series with capacity is used [11]. The value of the coil inductance is determined by the value of capacity in the way that it resonates on the resonant frequency of the transducer [7].

The properties of piezoelectric materials are described by following parameters [7]:

- **Electromechanical coupling coefficient** [-] – a ratio between the amount of the input mechanical energy and output electric energy. For a

reverse piezoelectric effect it is a ratio between input electric energy and output mechanical energy. It is described by a formula [9]:

$$k = \sqrt{\frac{Emechin}{Eelout}} \text{ or } k = \sqrt{\frac{Eelin}{Emechout}},$$

where *Emechin*, resp. *Emechout* is mechanical ene
Eelout is electrical energy.

- **Piezo-electric constants** – two constants that characterize a piezoelectric crystal as a receiver or transmitter of mechanical waves.

  d – piezo-electric module – a ratio between mechanical tension and electrical induction of applied electric field $\left[\frac{m}{V}\right]$; or the ratio between voltage and applied mechanic deformation.

  g – piezo-electric constant – the ratio between intensity of produced electric filed and mechanical deformation $\left[\frac{V}{m\,Pa}\right]$; or the ratio between deformation and applied electric induction.

- **Module of elasticity** $\left[\frac{N}{m^2}\right]$ – it can be described as [9]:

$$Y = \frac{mechanical\ pressure}{mechanical\ tension} \tag{3.2}$$

- **Density** $\left[\frac{kg}{m^3}\right]$ **–** the ratio between the mass and the volume [9]:

$$\rho = \frac{m}{V}, \tag{3.3}$$

- **Frequency constant** $[Hz \cdot m]$ – It is equal to half of the speed of propagation of the ultrasonic waves in a certain medium.. It can be computed using formula [3]:

$$N = f_r \cdot d\ , \tag{3.4}$$

where f_r is resonance frequency and *d* piezoelectric module.

- **Curie temperature** – if a piezoelectric material reaches this temperature, the piezoelectric properties are lost [3].

As it was discussed, all the crystals are anisotropic. Therefore each of those constants above must be followed by sign of the input and output plane. Sometimes, it is also followed by conditions of measurement. For example d_{33} means piezoelectric module measured for electric field applied in the plane perpendicular to axis 3 and mechanical deformations also measured in the plane perpendicular to axis 3. Table 1(later in the text) shows an example of values of the piezoelectric constants and other parameters characteristic for the PZT ceramics.

3.3.3 Sandwich transducer

Based on a function of regular ultrasonic transducer, there are more complicated structures called piezoelectric sandwich transducer. Usually, in stomatology the frequency range of ultrasonic waves is 25 – 50 kHz. The natural frequency of the piezoelectric element is higher than 100 kHz.

Formerly, the magnetostrictive transducers were used. Those transducers are based on dimension variation of a ferromagnetic material caused by external alternating magnetic field. Nevertheless, magnetostrictive transducers show worse electromechanical properties then piezoelectric transducers [11].

That was one of the reasons why sandwich transducers were developed. In connection with additional mass, a transducer with resonant frequency lower than 100 kHz can be built. The value of the resonant frequency of a sandwich structure is influenced by material and dimensions of additional mass.

The benefits of such construction are robustness, simple structure and low price. Furthermore, the additional mass provides cooling of the piezoelement by high thermal flux towards surface. Though during design of sandwich structure, it is impossible to consider all the negative effects, such as preload, material non-uniformity, acoustic coupling on junctions, etc. Therefore characteristics of a newly developed sandwich structure must be measured and accordingly adjusted in order to reach required behavior [11].

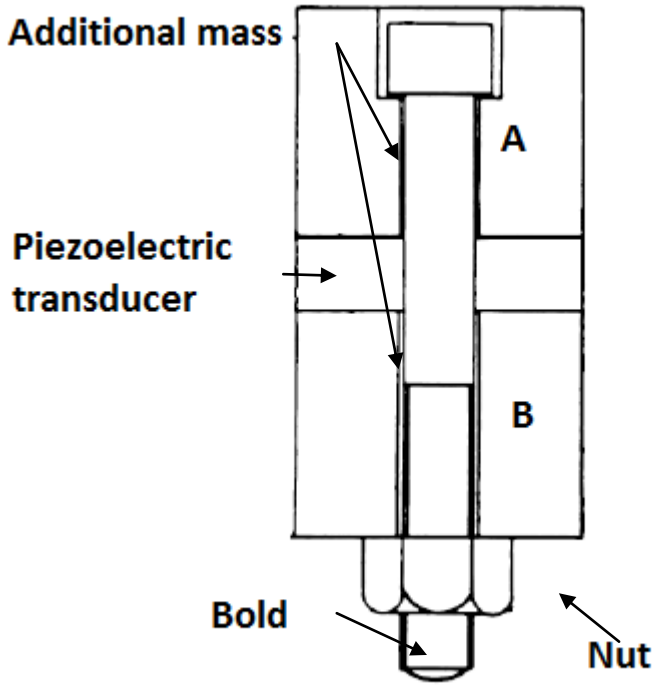

Fig. 3.6 Sandwich transducer structure

A composition of a sandwich transducer can be seen on Fig. 3.6. [11]. It consists of the basic piezoelement (with natural frequency higher than 100 kHz). This element is inset between two pieces of additional mass. Front additional mass (A) behaves as a quarter-wave transformer. This means that if we put it between generator and load, the acoustic impedance of load is transformed towards the generator output accordingly following formula [9]:

$$Z_{ef} = \frac{Z_a^2}{Z_z}, \tag{3.5}$$

where Z_a is acoustic impedance of the transformer (front mass) and Z_Z is acoustic impedance of load.

The acoustic impedance can be calculated as [3]:

$$Z = \rho \cdot v. \tag{3.6}$$

In practice, another unit for the acoustic impedance is used. It is Rayl, it is equal value of acoustic impedance 1 $Pa \cdot s \cdot m^{-1}$. Usually the value of acoustic impedance of real crystals is in the order of MRayls.

Hence the front mass can be used to match acoustic impedance of piezocrystal and impedance of load (waveguide). It exhibits in higher quality factor, better efficiency and more power delivered to load.

The rear additional mass (B, Fig. 3.6) causes “acoustic short”. Without additional mass, the transducer would radiate energy into both rear and front direction. In that case, the ultrasonic waves of front wave and reflected rear wave would interfere. In the extreme case it could cause annulations of both waves. The rear mass therefore helps to route as much energy as possible into load [11].

To maintain a good contact between crystal and additional mass, a thin layer of epoxide resin is applied on the junction. This compensates surface roughness of both junction parts. Although there has been a huge improvement is surface polishing during last few years, a resin layer is still being used on junctions [11].

Metal composite electrodes are used to connect power supply to piezo crystal. According to [11], the consistent electric contact of electrodes and crystal is achieved by use of net electrodes. They consist of net made of metal wire sunk in the epoxy resin. However it is really important to remove all the air bubbles which could appear on the junction during manufacturing. Firma Morgan Technical Ceramics co. is one of the main manufacturers, they use a 7,62 μm thick phosphor – bronze net with the density of electric eye 250/mm^2. By this combination a perfect contact between on junction electrode-crystal and additional mass-crystal is achieved.

In the most common construction of a sandwich transducer [3], all the above mentioned parts are drilled in the middle. This allows using a bold that provides mechanical compactness of structure and preload. The head of bold must be sunk in the material of the additional mass. Also a small adjustment of resonant frequency can be achieved by the mean of changing preload.

3.4 Material and dimensions of the piezoelectric transducer

The choice of transducer was based on materials provided in [8]. The product range of the Morgan Technical Ceramics co. is quite broad. Furthermore they offer some documents concerning piezomaterials and manufacturing of custom design

Basically, it is possible to choose of various types of zircon–titanate ceramics (PZT). According to manufacturer, materials are divided in two groups. The first group is called ceramics for low field. According to [13] this kind of ceramics is suitable for use in low electric fields, the sensitivity is rather high, but once it is used for power application, a significant heat loss appears.

The second group of materials seems to be more suitable for use in dental scaler. This group is called power PZT. It is capable to generate high intensity ultrasound waves; it has high quality factor and electromechanical coupling coefficient as high as 0,80. A commonly used ceramics is PZT – 5H that is suitable for general applications.

Another class of materials is signed PMN-PT –28. It is a family of newly developed material, which is composed of platinum-titanate monocrystal ceramics [7]. Obviously the exact composition of this material is not published. However in Table 1 [11], the main properties of PMNT-28 in comparison with standard ceramics are mentioned. The complete list of properties can be found in [11]. In Table 1 there are only those values that will be used later for design calculations. The electric and ultrasonic field will be oriented in the plane 3. Therefore the coefficients 33 are necessary for further computations.

In Table 1, we can see that the electromechanical coupling coefficient of PMN-PT-28 is about 15 % higher than of standard PZT. This allows improve efficiency of energy transfer which results in lower requirements for generator. PMN-PT-28 also has higher elasticity modulus, so the transducer can withstand higher mechanical load without damage. Therefore it is possible to reach higher acoustic power with just one piece of piezo-crystal. There is also small difference in the acoustic impedance of both compared materials. On the other hand, the Curie temperature of PMNT-28 is lower but it is still high enough for use in general applications

Price of the material is also one of the factors that need to be considered. The manufacturer guarantees that maximal difference of price in comparison with standard ceramics is 15%. The acoustic power of designed dental scaler is not so high, we can assume that only one piece of transducer will be used (this will be later proved by calculations). Therefore the price difference is not significant. Furthermore, lower electric power required on the output of generator may result in simple construction and lower cost. For this reason, the price of whole device with PMNT-28 crystal may be actually about the same as PZT crystal.

Table 1 Ceramic materials comparison

Property	PZT–5H	PMN–PT–28
k_{33}	0.75	0.86–0.90
d_{33} (pC/N)	690	1200–2000
g_{33} (x10^{-3} Vm/N)	19.7	15.8
$Y_{33}E$ (GPa)	4.8	25–30
Q_m	70	65
Frequency constant Nt (Hz·m)	2000	1800
Acoustic impedance (MRayl)	30	28
Density (kg/m^3)	7700	8100
Curie temperature (°C)	195	125–140

So the transducer will be made of PMN-PT-28 material. As it was mentioned above, there will be a bold in the middle of structure. It is useful to choose a ring transducer. It is useful to choose a transducer from product line because the properties of transducer are known and there is no need to carry out some measurements. Concerning dimensions, a transducer with the outer diameter D=14 mm and inner diameter d=6,5 mm may be used. Its natural resonant frequency is 450 kHz [11]. Then, we can calculate the width of transducer$[m]$:

$$d_m = \frac{N}{f}, \tag{3.7}$$

where N is frequency constant and f natural resonant frequency.

We can use values from Table 1:

$$d_m = \frac{N}{f} = \frac{1800}{450000} = 4\ mm \tag{3.8}$$

In the product line, there is one transducer having required width available. Schematic drawing can be seen on Fig.3.7 [8].

The product line table of Morgan Piezoelectrics is available in [8].

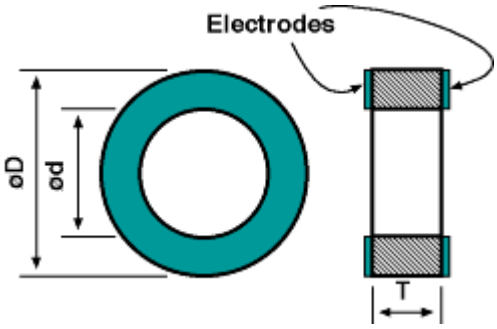

Fig. 3.7 Ring piezoelectric transducer

3.5 Additional mass and waveguide material

The choice of material of other parts of the ultrasonic system is the next step in design. In the previous chapter, the material of piezo-crystal was chosen. Therefore a suitable material for the front and rear additional mass and waveguide must be determined.

A practicable material must have good acoustic conductivity and appropriate elasticity modulus, so that the bonds between atoms are able to withstand high values of ultrasound intensity. Commonly used materials are titanium, steel, aluminum or alloys of all the mentioned [6].

If we assume that the toughness of material is sufficient, there are two more parameters that characterize the ultrasound wave propagation. The first one is (ρ) and the second one is the speed of propagation of ultrasound (v). Product of these parameters is acoustic impedance (equation 3.6). There may be a significant reflection on the boundary of two mediums with different acoustic impedance. Those reflections may cause decrease of efficiency of transfer of energy towards load and therefore lower output acoustic power.

In order to reach an optimal transfer of energy into a load, matching units must be used. Then, the boundaries are not so steep and the efficiency is acceptable [6].

To match acoustic impedance of piezocrystal and waveguide the front additional mass is used. As the mass of the tip is small in comparison with mass of waveguide, we can neglect it and consider waveguide as the load of transducer. The acoustic impedance of transducer is 28 MRayl (Table 1). With use of the equation 3.5 we can compute the quality of matching for various combinations of materials (3.5).

According to calculations, the best combination of materials appears to be following: front additional mass made of titanium and waveguide made of alumina AlCuMg2. That alloy is quite light high velocity of ultrasound wave propagation and sufficient toughness of waveguide.

For this combination with use of equations (3.5) and (3.6), the effective acoustic impedance was computed as:

$$Z_{ef} = \frac{Z_a^2}{Z_z} = \frac{(\rho_{Ti} \cdot v_{Ti})^2}{\rho_{Al} \cdot v_{Al}} = \frac{(4540 \cdot 4980)^2}{2780 \cdot 6100} = 30{,}14\ MRayl \qquad (3.9)$$

This value is the closest one to the value of the acoustic impedance of the transducer 28 MRayl. Of course there is never a perfect matching; the properties of real materials may be slightly different or inhomogeneous

The material composition of designed structure is following:

Titanium rear additional mass– piezoelectric transducer PMN–PT–28 – titanium front additional mass –alumina alloy waveguide

3.6 Waveguide design

Before we get to the sandwich structure design, it is necessary to calculate dimensions of the acoustic waveguide. The waveguide is used to reduce the diameter of applicator towards the tip. Furthermore, the amplitude of ultrasonic waves is amplified. The ratio of amplification depends on the coefficient of amplification. With the same electric power, the structure with waveguide can reach higher ultrasound intensity [4].

There are three commonly used shapes of waveguide [4]:

1) Conical waveguide (Fig. 3.8a) – the theoretical coefficient of amplification [-] depends on the length of waveguide [3]:

$$K = \sqrt{1 + (k \cdot l)^2}, \tag{3.10}$$

where *k* is wave number and *l* length of the waveguide.

The theoretical coefficient of amplification is ever smaller than the ratio of diameter of waveguide at the beginning and at the end (D_0 / D_1). The advantages are simple shape and therefore lower price. On the other hand the conical waveguide has higher volume and mass. It is suitable for simple applications with emphasis on price and ease of manufacturing.

2) Exponential waveguide (Fig 3.8b) – the theoretical coefficient of amplification [-] depends on diameter of waveguide at the beginning and at the end. It can be computed as [3]:

$$K = \frac{D_0}{D_1}, \tag{3.11}$$

where D_0 is diameter of the waveguide at the beginning and D_1 diameter of the waveguide at the end.

3) Catenoidal waveguide (Fig. 3.8c) – the contour line is called catenoid. Mathematically it is defined as hyperbolic cosine. The theoretical coefficient of amplification [-] depends on the length of waveguide and wave number. It is known that the value is higher than the ratio of diameters [3]:

$$K > \frac{D_0}{D_1}. \tag{3.12}$$

The exact formula for computing of value of the coefficient of amplification of catenoidal waveguide can be found in [4]. If we have a look at the shape of this waveguide Fig. 3.8, we can see that the diameter of waveguide is rapidly decreasing at the beginning and then it is nearly constant. In addition to large coefficient of amplification, it may be used for applications where small constant diameter and long waveguide are required. For example, it is often used for ultrasonic percutaneous extraction of urinary calculi. For this, the applicator with the length of about 40cm must be placed inside of a catheter with diameter of few millimeters.

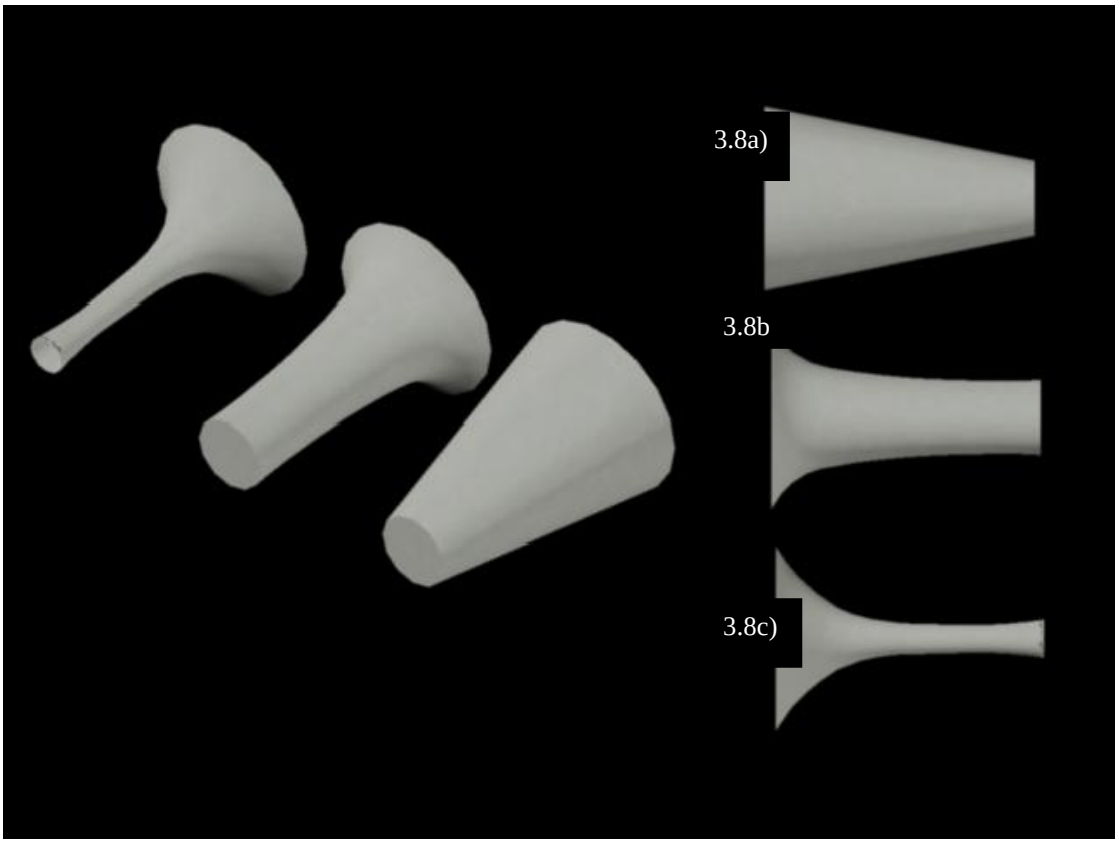

Fig. 3.8 Waveguide types: a) conical waveguide, b) exponential waveguide, c) catenoidal waveguide

The exponential waveguide appears to be suitable for the construction of ultrasonic dental scaler. It is lighter than the conical waveguide and price is not higher than 10% [14]. There are no further dimension requirements.

Once the type of waveguide is chosen, computation of its dimensions can be done. The mass of waveguide is connected to the front mass of transducer with diameter 14mm. At the end, the working tip is screwed into the mass of waveguide. The dimensions were computed for standard tips manufactured by Amdent co.. As can be seen on Fig. 3.2, the diameter of tip is 6mm. In the middle of waveguide, there is a duct used for transporting water towards tip. The diameter of the duct is 1mm. As the diameter of the duct is small in comparing to the diameter of waveguide, the effect of the duct on ultrasound wave propagation is negligible. The whole structure of applicator is pictured on Fig. 3.9.

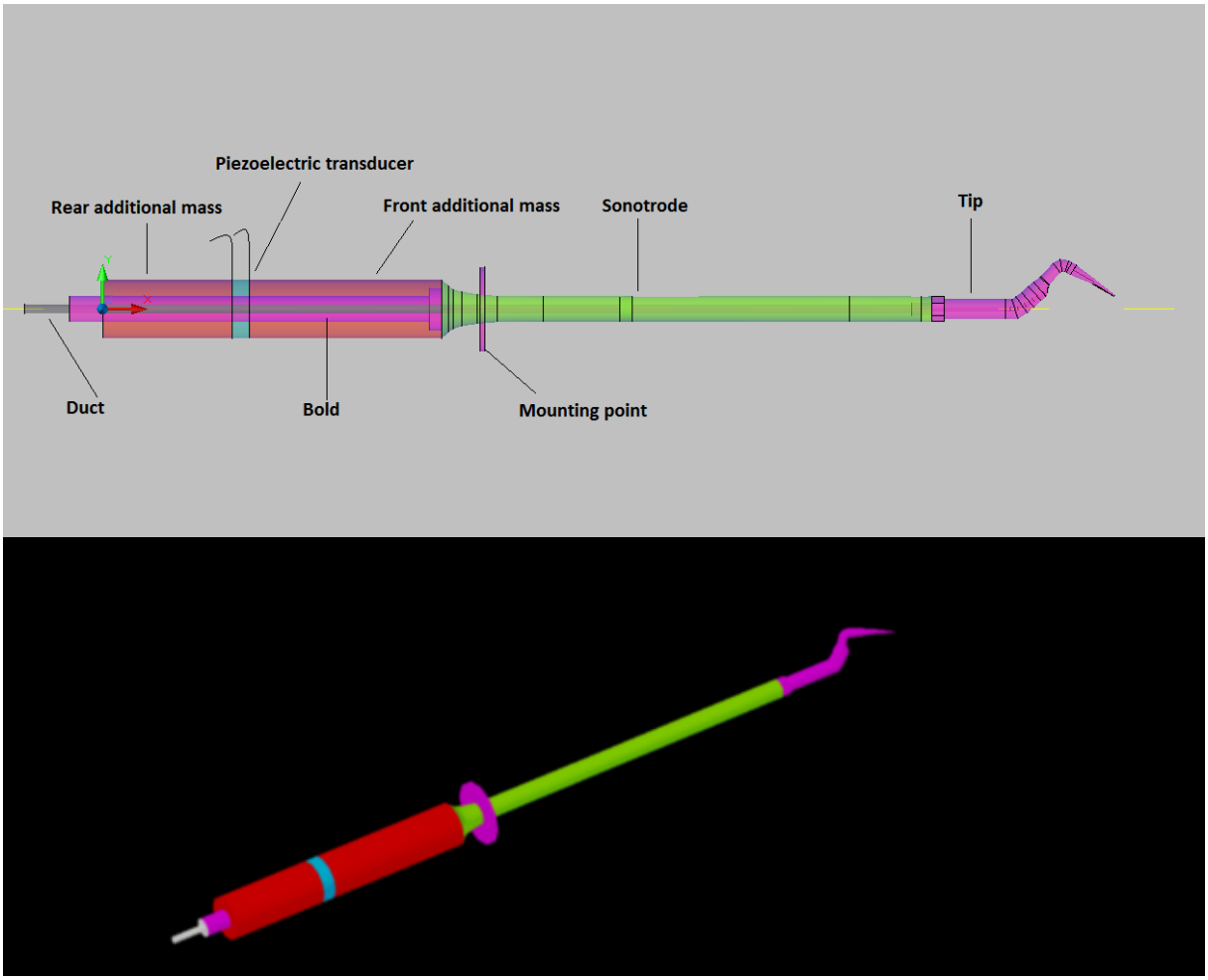

Fig. 3.9 Applicator structure

The last step is calculation of the waveguide length. Usually half-wavelength waveguides (the length is n-times higher than half of the length of the wave of ultrasound) are used [9]. In real applications, the length of waveguide is usually a bit higher than calculated. A waveguide like that is supposed resonate on the frequency corresponding to the frequency of transducer. As it is desirable to keep the dimensions of applicator compact, the waveguide with the length of one times half wavelength is used. A graphic method may be used to calculate dimensions. Two diagrams are used (Fig. 3.10).

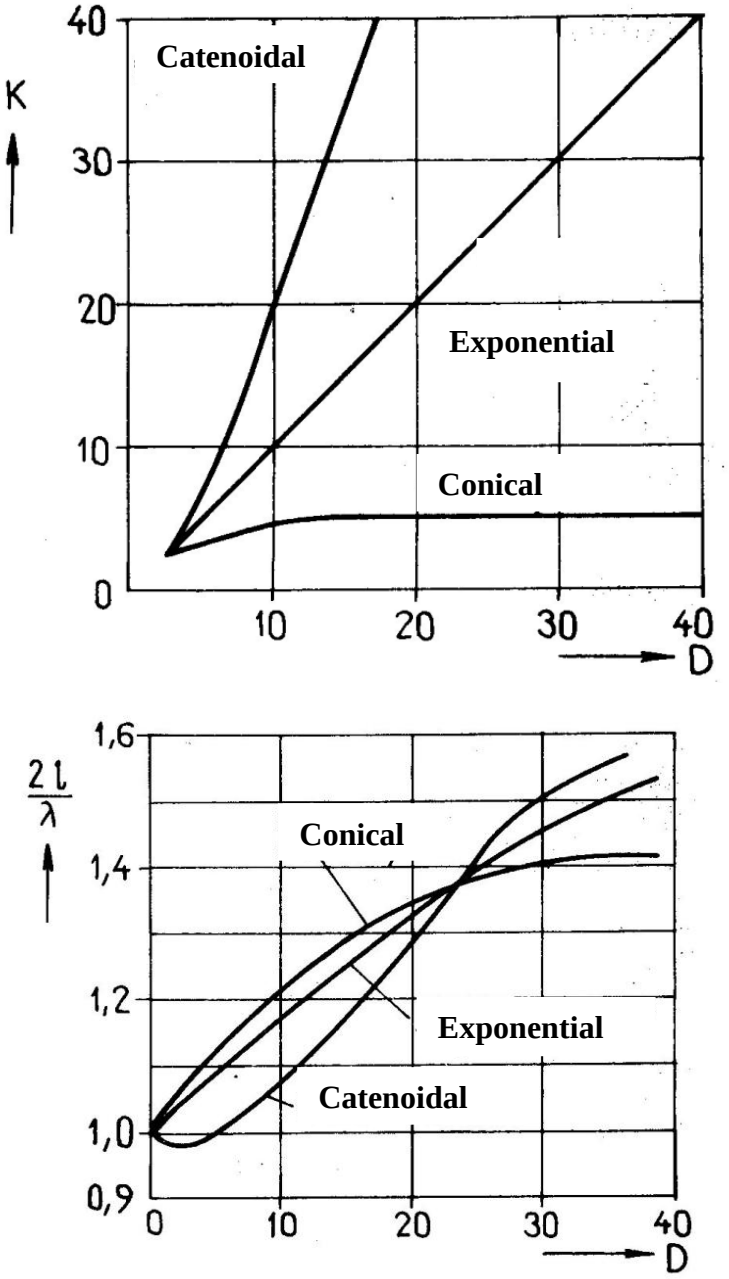

Fig. 3.10 Waveguide characteristics

For above mentioned diameters the coefficient of amplification can be computed:

$$K = \frac{D_0}{D_1} = 2{,}33. \tag{3.13}$$

For that value of *K*, we can obtain value of D=2,5 with use of plot on Fig. 3.10. Then with use of the second plot on Fig. 3.10, we get value of the ratio $\frac{2l}{\lambda}$ = 1,03.

From that equation, the length of waveguide can be derived [3]:

$$l = \frac{\lambda}{2} \cdot \mathrm{m} = \frac{v}{2 \cdot f} \cdot \mathrm{m}\,, \tag{3.14}$$

where λ is wavelength, v is the velocity of propagation of ultrasonic waves and f frequency of waves. For working frequency 27 kHz and velocity of propagation in waveguide material 6320 $m \cdot s^{-1}$ we get:

$$l = \frac{6320}{2 \cdot 27000} \cdot m = 0{,}120\, m = 120\, mm. \tag{3.15}$$

3.7 Sandwich transducer calculation

In the last step, the dimensions of additional mass of the sandwich structure have to be computed.

The calculation is based on equations that were created by Paul Langevin, the inventor of sandwich transducer [9].

To calculate dimensions following equation can be used [9]:

$$\frac{\omega l_c}{v_c} + tg^{-1} \frac{S_a \rho_a v_a}{S_C \rho_C v_C} tg \frac{\omega l_a}{v_a} + tg^{-1} \frac{S_b \rho_b v_b}{S_C \rho_C v_C} tg \frac{\omega l_b}{v_b} = \pi \tag{3.16}$$

where

l_a, l_b, l_C……is the length of front additional mass, rear additional mass and piezoelectric transducer (m);

v_a, v_b, v_C…….. is velocity of ultrasound propagation in each section (m/s);

S_a, S_b, S_C... is cross section of each section (m^2);

ρ_a, ρ_b, ρ_C….is the density of material of each section (kg/m^3).

For real calculations a simplified equation can be used [3]. The process of calculation is following:

$$tg \frac{2 \cdot \pi \cdot l_c}{\lambda_c} \cdot tg \frac{2 \cdot \pi \cdot l_b}{\lambda_b} = \frac{\rho_c \cdot v_c}{\rho_b \cdot v_b}. \tag{3.17}$$

We assume that the diameter of transducer and additional mass are the same, the width of the front additional mass is quarter-wavelength:

$$l_a = \frac{\lambda_a}{4} = \frac{v_a}{4 \cdot f}. \tag{3.18}$$

For the frequency 27 kHz and titanium additional mass we get:

$$l_a = \frac{4980}{4 \cdot 27000} = 0{,}046\, m = 46\, mm. \tag{3.19}$$

The width of the rear additional mass can be calculated with use of the equation (3.17) that can be modified as:

$$cotg\,\frac{\omega_s.l_c}{v_c} = \frac{\rho_b \cdot v_b}{\rho_c \cdot v_c} \cdot tg\,\frac{\omega_s \cdot l_b}{v_b}. \tag{3.20}$$

For better transparency of calculation a substitution is used [3]:

$$\gamma_c = \frac{\omega_s.l_c}{v_c}, \tag{3.21}$$

$$m = \frac{\rho_b \cdot v_b}{\rho_c \cdot v_c}, \tag{3.22}$$

$$\gamma_b = \frac{\omega_s.l_b}{v_b}, \tag{3.23}$$

Then we get the equation (3.20) in the form:

$$cotg\ \gamma_c = m \cdot tg\ \gamma_{b.} \tag{3.24}$$

Next, another substitution is used:

$$tg\ \beta_b = m \cdot tg\ \gamma_b. \tag{3.25}$$

With use of the equation (3.24) we get:

$$tg\ \beta_b + tg\ (\gamma_c + \tfrac{\pi}{2}) = 0. \tag{3.26}$$

When the argument of the tangent function is small:

$$tg\ (x) = x. \tag{3.27}$$

Then for $n \in Z$:

$$\beta_b + \gamma_c + \frac{\pi}{2} = n \cdot \pi. \tag{3.28}$$

Or we can transform it into:

$$\beta_b + \gamma_c = (2 \cdot n - 1) \cdot \tfrac{\pi}{2}. \tag{3.29}$$

With use of set values in equation (3.22), we get the ratio of acoustic impedance:

$$m = \frac{4540 \cdot 4980}{8100 \cdot 3450} = 0{,}809. \tag{3.30}$$

From the equation (3.21) we calculate parameter γ_c:

$$\gamma_c = \frac{2 \cdot \pi \cdot 27000 \cdot 0{,}004}{3450} = 0{,}197, \tag{3.31}$$

and from the equation (3.29) parameter β_b for n = 1:

$$\beta_b = \frac{\pi}{2} - \gamma_c = 1{,}570 - 0{,}197 = 1{,}374. \tag{3.32}$$

Further, from the equation (3.19) the parameter γ_b is computed :

$$\gamma_b = cotg\,\frac{\beta_b}{m} = cotg\,\frac{1{,}374}{0{,}809} = 1{,}039. \tag{3.33}$$

Finally, the width of the rear additional mass is calculated with the use of the equation (3.23) as:

$$l_{\mathrm{b}} = \frac{\gamma_b \cdot v_b}{2 \cdot \pi \cdot f} = \frac{1{,}039 \cdot 4980}{2 \cdot \pi \cdot 27000} = 0{,}031\ m = 31\ mm. \tag{3.34}$$

Once the structure is manufactured, there may be some additional adjustments needed, as the properties of the real material may be slightly different.

The resonant frequency can be also adjusted by preload caused by the bold. The bold is made of titanium, the outer diameter is 6mm and there is a bore with a diameter 2,1mm. A pipe leads inside that bore. The pipe is ended up with thread that allows connection to water inlet.

For mechanical construction, it is important to calculate the mounting point. It is used to mechanically connect applicator with its plastic case. The best location of that mounting point is on the place where there is a node of ultrasonic waves. Therefore the amplitude of oscillation in this place is minimal and oscillations do not propagate through case towards dentist's hand [1]. If the position of the mounting point is not correct, the surface of the device oscillates and also part of the acoustic power is lost.

The location of the mounting point can be found with the use of following equation [3]:

$$x = \frac{l}{\pi} \cdot arctg\left(\frac{1}{\pi}\right) \cdot \ln\left(\frac{D_0}{D_1}\right), \tag{3.35}$$

where l is the length of waveguide, D_0 diameter of the front side of the waveguide and D_1 is the diameter of the rear side of the waveguide. And we can calculate:

$$x = \frac{0{,}117}{\pi} \cdot arctg\left(\frac{1}{\pi}\right) \cdot \ln\left(\frac{0{,}014}{0{,}006}\right) = 0{,}0097\ m = 9{,}7\ mm. \tag{3.36}$$

The location of the mounting point is 9,7 mm from the front part of waveguide.

Next, the theoretical coefficient of amplification can be determined with the use of the equation (3.11):

$$K = \frac{0{,}014}{0{,}006} = 2{,}33. \tag{3.37}$$

4. Generator output power calculation

Once the structure of the applicator is designed, the output power of the generator can be computed. The maximal ultrasound intensity of 5 W/cm^2 at the working tip is required. As the mass of the tip is small in comparing to mass of the rest of applicator, we can assume that required value of intensity is also at the end of waveguide. So it is necessary to calculate the value of intensity towards the generator.

The ultrasound intensity determines the power in a unit area. It can be expressed by the equation [4]:

$$I = \frac{1}{2} \cdot \rho \cdot v \cdot \omega^2 \cdot U^2 \,, \tag{4.1}$$

where ρ is the density of the medium, v is velocity of ultrasonic waves propagation, ω is the angular velocity and U is the amplitude of ultrasonic oscillations.

As it was mentioned, the waveguide amplifies the magnitude of oscillations K-times. So it is necessary to calculate the magnitude of oscillations at the end of the waveguide with use of the equation (3.25):

$$\begin{aligned} U &= \sqrt{\frac{2 \cdot I}{\rho \cdot v \cdot (2 \cdot \pi \cdot f)^2}} \\ &= \sqrt{\frac{2 \cdot 50000}{2700 \cdot 6320 \cdot (2 \cdot \pi \cdot 27000)^2}} = \\ &= 4{,}51 \cdot 10^{-7}\text{m} = 0{,}451\ \mu m. \end{aligned} \tag{4.2}$$

The coefficient of amplification expresses ratio of magnitude of input and output ultrasonic waves [3]:

$$K = \frac{U_{out}}{U_{in}}. \tag{4.3}$$

Then we can calculate the magnitude of the ultrasonic waves at the beginning of waveguide:

$$U_{in} = \frac{U_{out}}{K} = \frac{0{,}451 \cdot 10^{-6}}{2{,}33} = 0{,}194 \cdot 10^{-6} = 0{,}194\ \mu m. \tag{4.4}$$

And reciprocally the intensity of ultrasound at the beginning of waveguide can be computed of the equation (4.1):

$$I_{in} = \frac{1}{2} \cdot 2700 \cdot 6320 \cdot (2 \cdot \pi \cdot 27000)^2 \cdot (0{,}194 \cdot 10^{-6})^2 = 9241 \frac{W}{m^2} = 0{,}9241 \frac{W}{cm^2} \tag{4.5}$$

In the ideal case, we can assume that the front additional mass behaves as quarter-wavelength transformer and transfer all the acoustic power towards the load. Then the intensity of ultrasound at the end of front additional mass is equal to the intensity of ultrasound produced by the piezoelectric transducer itself (I_m) [4]:

$$I_{in} \cong I_m. \tag{4.6}$$

The acoustic power P_m of the transducer can be calculated as:

$$P_m = I_m \cdot S_m, \tag{4.7}$$

where S_m is the active area of the ring transducer, which is (D is outer diameter and d is inner diameter):

$$S_m = \pi \cdot \left[\left(\frac{D}{2}\right)^2 \cdot \left(\frac{d}{2}\right)^2\right] = \pi \cdot \left[\left(\frac{0{,}014}{2}\right)^2 - \left(\frac{0{,}0065}{2}\right)^2\right] = 1{,}21 \cdot 10^{-4}\ m^2. \tag{4.8}$$

Next, we get the required acoustic power of the transducer:

$$P_m = 9241 \cdot 1{,}21 \cdot 10^{-4} = 1{,}12\ W \tag{4.9}$$

The conversion of electric energy into mechanical energy is characterized by the electromechanical coupling coefficient (P_{el} is input electric power of the transducer) [3]:

$$k_p = \frac{P_m}{P_{el}}, \tag{4.10}$$

with the value from the Table 1 we get:

$$P_{el} = \frac{P_m}{k_p} = \frac{1{,}12}{0{,}86} = 1{,}30\ W. \tag{4.11}$$

There are coupling circuits between generator and transducer. The efficiency of these circuits is however not 100%. Usually the range of efficiency is 0,80 – 0,85 [1]. The output electric power of the generator is [4]:

$$\eta = \frac{P_{el}}{P_{gout}}, \tag{4.12}$$

where P_{gout} is the output electric power of the generator.

Then:

$$P_{gout} = \frac{P_{el}}{\eta} = \frac{1{,}30}{0{,}80} = 1{,}625\ W. \tag{4.13}$$

As we know the value of required electrical power, we can compute the value of voltage from the equation:

$$U = \sqrt{P \cdot R}\,, \tag{4.14}$$

where R is the real part of the impedance. When the transducer works on the resonant frequency the value of impedance is 75 Ω [8].

Finally we get the driving voltage of transducer:

$$U = \sqrt{1{,}625 \cdot 75} = 11\ V \tag{4.15}$$

5. Design of electronic circuits

In this chapter, the design of all the electronic circuits of the dental scaler device is described step by step. It includes the diagrams of connection of the generator, the power supply and the digital control block.

5.1 Generator

As it was mentioned before, the ultrasonic transducer is driven by a sine wave generator. The block of the generator consists of an oscillator, amplifier and matching circuit. It must provide sufficient values of voltage and current at the output. These values were calculated in the previous chapter.

5.1.1 Oscillator

There are many kinds of circuitry which can produce a sine wave signal. Generally oscillator can be built of discrete devices (Wien oscillator, three point oscillator, etc.) or an integrated circuit can be used. The examples of discrete-devices circuits can be found in [3].

However as the price of the integrated circuits has decreased in recent years, they can become more efficient than the discrete device version. There are some simple integrated circuits such as versions of the "555" circuit. However for the design of the dental scaler, a more sophisticated device was chosen. As the oscillator, the integrated circuit XR-220, signed as monolithic function generator, was used.

The advantage is that the parameters of the generated sine wave, such as amplitude and frequency, can be easily changed with use of few external resistors. It also allows producing triangle, ramp and square waveform. Then the generator can be easily redesigned for different applications than dental treatments. The frequency can be set in the range 0,01 Hz- 1 Mhz. The output amplitude can be up to 6V [12].

The Table 2 shows the pin description of the XR-2206. On the picture *Fig. 5.1* the connection as sine wave generator is shown. The connection follows recommendation from datasheet. According to the datasheet [12], the minimal supply voltage is 10V. For this reason, the circuit was connected to 18V power supply. That supply will be also used later for the amplifier. The capacitor C2 is used to block voltage ripple coming from the power supply leads.

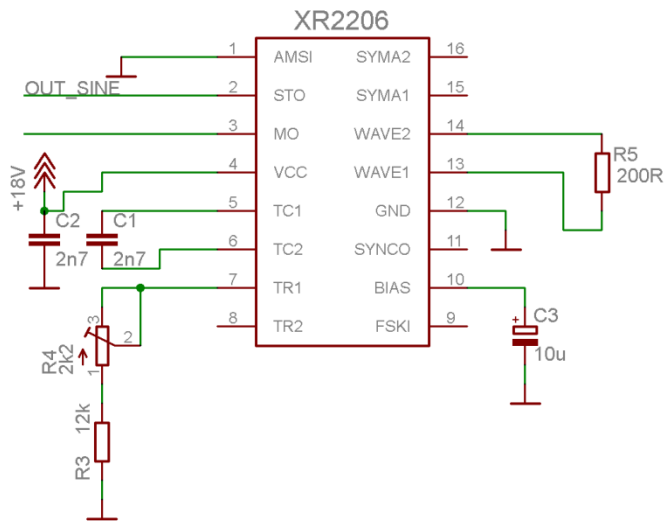

Fig. 5.1 Oscillator integrated circuit connection diagram

The output frequency can be set by the capacitor C1 (connected between pins 5 and 6) and a resistor R connected to pin 7. The formula for calculating frequency [Hz] is [12]:

$$f = \frac{1}{R \cdot C_1}. \tag{5.1}$$

The value of the resistor *R* should be in the range 4kΩ - 200kΩ. Accordingly, the value of the capacitor *C1* can be chosen as 2,7nF.

The value *R* [Ω] can be calculated from the equation 5.1:

$$R = \frac{1}{f \cdot C_1}, \tag{5.2}$$

where f is the working frequency and C_1 known capacity.

Then we can substitute the known values and calculate *R*:

$$R = \frac{1}{27000 \cdot 2{,}7 \cdot 10^{-9}} = 13717\Omega. \tag{5.3}$$

As the value is quite precise, it would not be easy to get this resistance with use of the standard resistance values series. Therefore it is useful to use a serial connection of resistor and potentiometer (R3 and R4 on Fig. 5.1). This way the exact value can be set to adjust frequency.

To generate sine wave, there must be a 200 Ω resistor connected between pins 13 and 14 [12]. The pin 10 is connected via an electrolytic capacitor to the ground. Pin number 2 is the output connected to the amplifier.

To adjust amplitude, there is a resistor used connected between the pin number 3 and ground. The value of the resistor can be derived from the diagram on Fig. 5.2. For the chosen peak output voltage 3V, the 50kΩ R3 is needed [12].

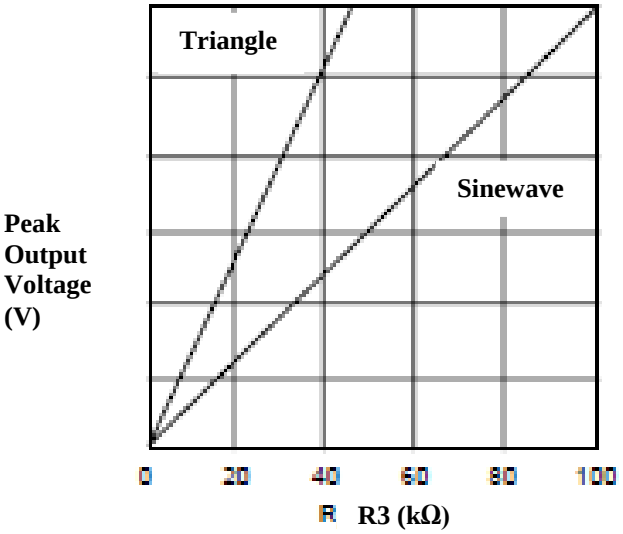

Fig. 5.2 Oscillator integrated circuit connection diagram

As there is a need to change the intensity of the ultrasound stepwise, the digital potentiometer is used (Fig.5.3). It includes internal switches which allow changing the resistance in 64 steps (MCP4011). The potentiometer communicates with the microprocessor via a serial line (MOSI and CS_POT signals). The MOSI signal is the serial line connection and CS_POT is used as chip select. The analog potentiometer R8 is used for fine adjustment of the R3 middle value and position of the resistance steps. The potentiometer is connected to 5V supply according to datasheet [13]. Pin number 6 is connected to the XR2206.

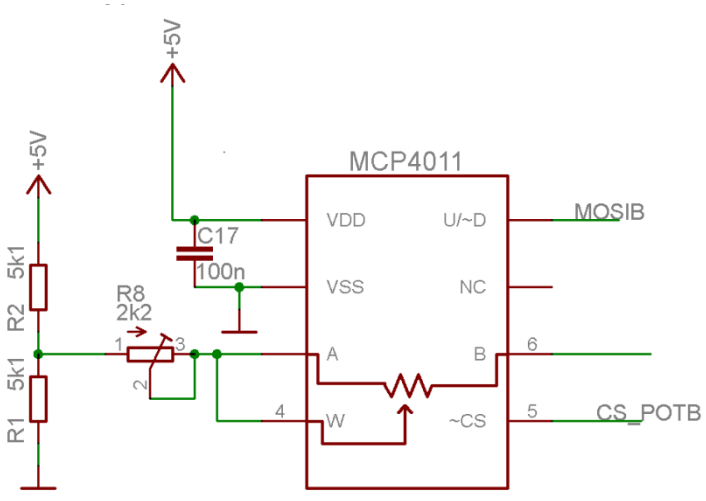

Fig. 5.3 Digital potentiometer connection diagram

5.1.2 Amplifier

The signal generated by the oscillator has to be amplified to the value needed for driving the transducer. There are again two ways how to design it. An amplifier built of

discrete transistors or integrated circuit can be used. As the requirements (low amplification, distortion and bandwidth) for the amplifier are not very demanding in this case, an operational amplifier can be used.

In the previous chapter, the value of voltage to be produced by generator is 11V. This value is effective voltage. As the oscillator produces sine wave with the amplitude of 3V, it must be recalculated to effective value according to the common formula:

$$U_{ef} = \frac{U_{max}}{\sqrt{2}}. \tag{5.4}$$

Then:

$$U_{ef} = \frac{3}{\sqrt{2}} = 2{,}12V. \tag{5.5}$$

For the choice of a suitable operational amplifier, the value of current [A] flowing to transducer must be estimated. We can assume that in resonance, the impedance of the transducer has a real value. The value is 75Ω [8]. Then the simple estimation can be used by applying the Ohm's law:

$$I = \frac{U}{R}. \tag{5.6}$$

So we get:

$$I = \frac{11}{75} \cong 147\ mA. \tag{5.7}$$

The output current for a general purpose operational amplifier is usually less than 100mA. Then, a current driver would have to be designed to provide enough output current for the transducer.

However, a high output current amplifier can be used. A suitable amplifier in this category is OPA552 [17]. The continuous output current is 200mA, which is according to calculation in the equation 5.7 sufficient. The supply voltage range is ±4V to ±30V. As we need 11V RMS on the transducer, the amplitude is:

$$U_{max} = U_{RMS} \cdot \sqrt{2} = 11 \cdot \sqrt{2} = 15{,}56V. \tag{5.8}$$

According to the datasheet [17], the output swing is 2V from rail. That means that the minimal supply voltage must be 17,56V. The ±18V symmetrical power supply can be therefore used.

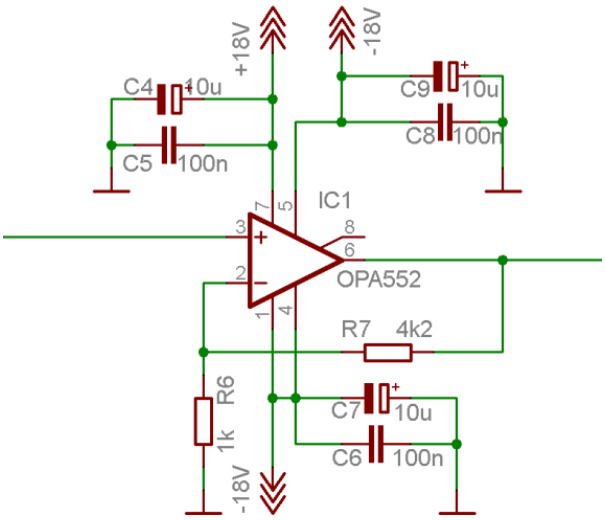

Fig. 5.4 Amplifier connection diagram

The power supply leads are filtered by parallel combination capacitors with capacities 10μF and 100nF. The OPA522 amplifier is optimized for gains 5 or greater. The required gain can be calculated as a ratio of input and output voltage (values from equations 4.15 and 5.3):

$$A = \frac{U_{out}}{U_{in}} = \frac{11}{2{,}12} = 5{,}19. \tag{5.9}$$

As the operational amplifier is connected as non-inverting amplifier, the gain is determined by the values of the resistors R6 and R7 in the feedback loop (Fig.5.4). If we chose the value of R6 1kΩ, we can calculate the value of R7 with use of formula for non-inverting amplifier gain *A* [-]:

$$A = 1 + \frac{R7}{R6}. \tag{5.10}$$

Then for *R7*:

$$R7 = R6 \cdot (A - 1) = 1000 \cdot (5{,}19 - 1) = 4190\Omega. \tag{5.11}$$

Therefore the value of the resistor R7 is 4200Ω.

5.1.3 Matching circuit

The matching circuit is used to deliver as much power into load as possible. When the output impedance of the amplifier differs from the impedance of the load, a significant part of the power reflects and therefore does not propagate into the load [3].

Usually, a resonant circuit is used to drive a transducer. This is derived from the substitution diagram of a piezoelectric transducer (Fig. 3.4). The right branch of the diagram is called motion impedance. This impedance characterizes the transducer in resonance. The other branch consists of the real resistance of the dielectric and C0 is the static capacity of the transducer. Therefore a resonant circuit with inductance can be used to tune the transducer into resonance. As the resonant frequency of the transducer

depends on the output impedance of the generator, the more sophisticated circuits are commonly used (Fig. 5.5) [15]. The easiest way for construction is the circuit b), because there is no need for inductance coupling or any special coils. This circuit was also used in this project. The real connection diagram can be seen on Fig. 5.6.

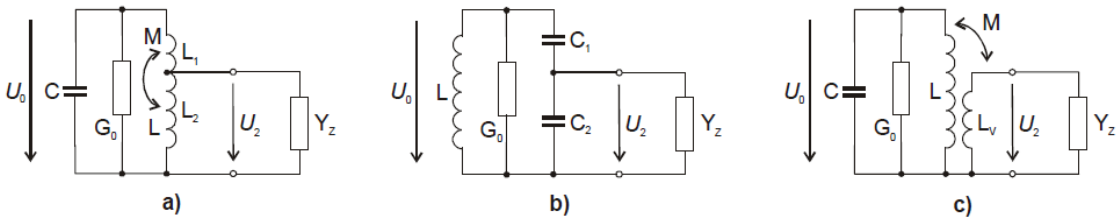

Fig. 5.5 Matching circuits a) Inductive coupling b) Capacitive coupling c) Transformer coupling

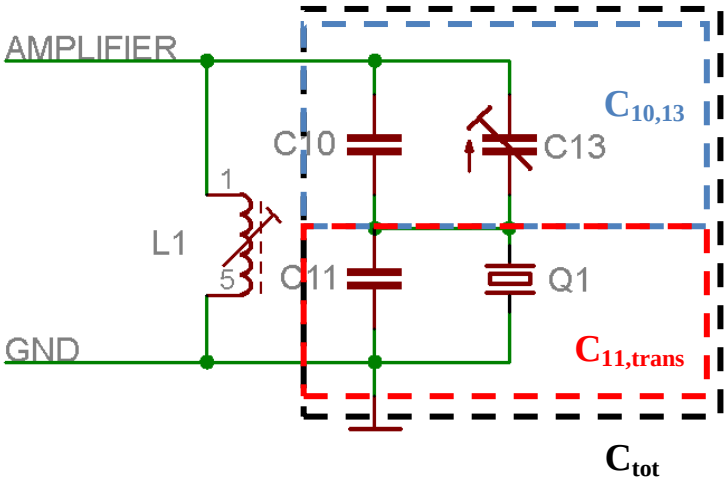

Fig. 5.6 Theoretical matching circuit connection diagram

There is an effort to tune the static capacity of the transducer into resonance. The static capacity [F] can be calculated from the dimensions of the transducer using common formula:

$$C_0 = \varepsilon_0 \cdot \varepsilon_r \cdot \frac{S}{d}, \tag{5.12}$$

where ε_0 is permittivity of vacuum, ε_r relative permittivity of dielectric, S is the area of the transducer and d thickness of the transducer.

The permittivity of dielectric for the chosen transducer is 2400 [8]. The area of transducer has been already calculated from the equation 4.8 as $1{,}21 \cdot 10^{-4}$ m^2. The thickness of transducer is 4mm.

Then we can calculate:

$$C_0 = 8{,}86 \cdot 10^{-12} \cdot 2400 \cdot \frac{1{,}21 \cdot 10^{-4}}{4 \cdot 10^{-3}} = 643\ pF. \tag{5.13}$$

It must be considered that the transducer is connected to the matching circuit via a coaxial cable. A suitable coaxial cable is 179 B/U [16] with resistance of 75Ω (the

same value as the resistance of the transducer) and the specific capacity 19,6 pF/m. For a 2 meters long cable we get capacity [16]:

$$C_{coax} = l \cdot C = 2 \cdot 19{,}6 = 39{,}2\ pF, \tag{5.14}$$

where *l* is the length of the cable and *C* specific capacity.

The capacity of the cable is connected parallel to the capacity of the transducer. So the total capacity of transducer and cable is:

$$C_{trans} = C_{coax} + C_0 = 39{,}2 + 643 = 682{,}2\ pF. \tag{5.15}$$

We can use Thomson formula to calculate value of capacity and inductance needed to keep the circuit on resonant frequency 27 kHz [14]:

$$\omega = \frac{1}{\sqrt{L \cdot C}}. \tag{5.16}$$

Thus:

$$C = \frac{1}{(2 \cdot \pi \cdot f)^2 \cdot L}. \tag{5.17}$$

An adjustable coil 126ANS-T1096Z was chosen. This coil is adjustable in the range of 1-15 mH. We assume that the inductance is set to 10 mH. The capacity C_{tot} can be calculated with use of the equation 5.17:

$$C_{tot} = \frac{1}{(2 \cdot \pi \cdot 27000)^2 \cdot 10 \cdot 10^{-3}} = 3{,}474\ nF. \tag{5.18}$$

If we choose capacity C_{11} (Fig. 5.7) as 3,9 nF, then the capacity of parallel connection of C_{11} and C_{trans} is:

$$C_{11,trans} = C_{11} + C_{trans} = 3{,}9 \cdot 10^{-9} + 682{,}2 \cdot 10^{-12} = \tag{5.19}$$

$$= 4{,}5822\ pF.$$

Once the values of capacities $C_{11,trans}$ and C_{tot} are known, the capacity $C_{10,13}$ can be computed as (the $C_{11,trans}$ and $C_{10,13}$ are in series connection):

$$C_{10,13} = \frac{C_{tot} \cdot C_{11,trans}}{C_{11,trans} - C_{tot}}. \tag{5.20}$$

If we substitute the values, we get:

$$C_{10,13} = \frac{3{,}474 \cdot 10^{-9} \cdot 4{,}582210^{-9}}{4{,}582210^{-9} - 3{,}474 \cdot 10^{-9}} = 14{,}36\ \text{nF}. \tag{5.21}$$

The capacity can consist of set of parallel connected capacitors, which addition of their capacities will be equivalent to the computed $C_{10,13}$ capacity. For tuning of the circuit, some of the capacitors must be adjustable.

So finally the capacity $C_{10,13}$ is created of parallel combination of three capacitors with capacities 12 nF; 1,8 nF; 390 pF; and an adjustable capacitor. On the printed circuit board there will be three footprints for capacitive trimmers to allow experimental tuning, if necessary. This combination allows to change the capacity within the range of 14,21 – 14,46 nF, see Fig. 5.7.

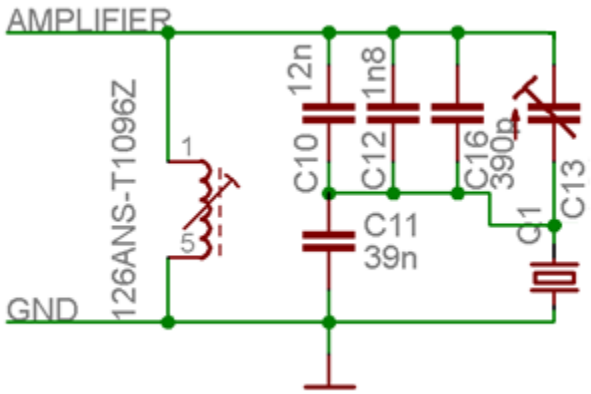

Fig. 5.7 Real matching circuit connection diagram

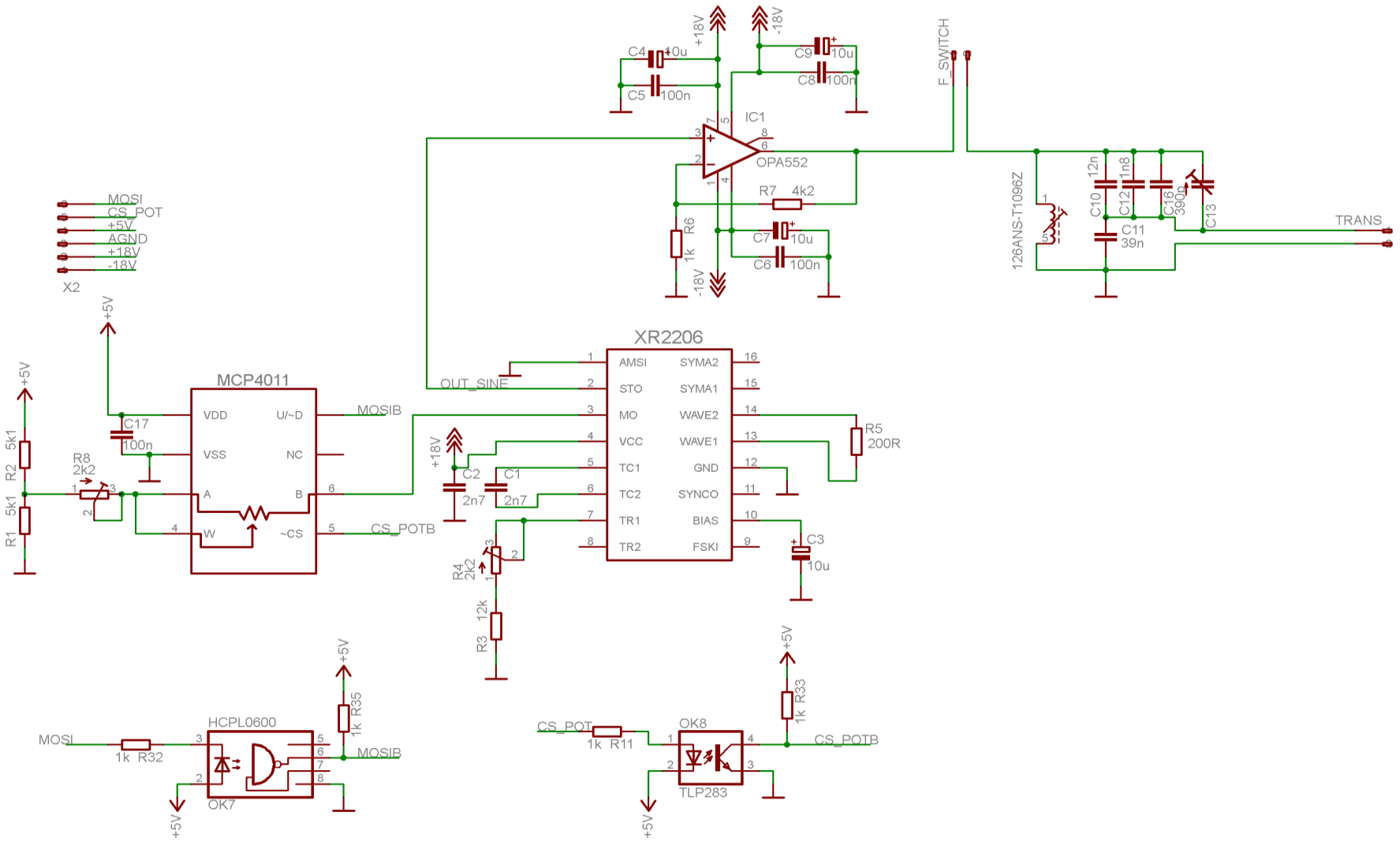

Fig. 5.8 Generator connection diagram

5.1.4 Connection diagram of generator

There is a complete connection diagram of the generator part on Fig. 5.8. As there is a need to separate analog and digital ground, the digital signals MOSI and CS_POT coming from the microprocessor are separated by optocouplers with phototransistors. As the bandwidth of the optocoupler TLP283 is not wide enough to transmit the MOSI signal, the HCPL0600 optocoupler is used instead.

There are two connectors in the diagram. The first one F_SWITCH is connected to the foot switch. Once it is pressed, the switch is on and the output of the generator is connected to the applicator.

The second connector X2 is used to connect the generator to the power supply and to the digital signals from microprocessor.

5.2 Digital control circuits

5.2.1 Microprocessor

As the main part of the control circuits, the microcontroller ATMEGA 64-A is used. It is an 8-bit microcontroller with 64kB of build-in reprogrammable flash memory. The pin description can be seen on Fig. 5.9. According to [18], the microcontroller is connected as it is shown on Fig. 5.10.

The microcontroller is connected to the 5V power supply. There is a 16 MHz quartz crystal creating a clock signal for the circuit. The voltage on the pin RESET is held on the high level with external pull-up resistor R7. The function of the other connections will be described later. There are two LED diodes connected to pins 25 and 26, which are used for signalizing of error states and output function. On the pin 32 the piezoelectric buzzer F/CM12P is connected [26].

There is a connector for ISP (in system programming), which allows the microcontroller to be reprogrammed via a serial interface directly on the printed board circuit. The connection is made according to [18]. The connection diagram can be seen on Fig.5.9.

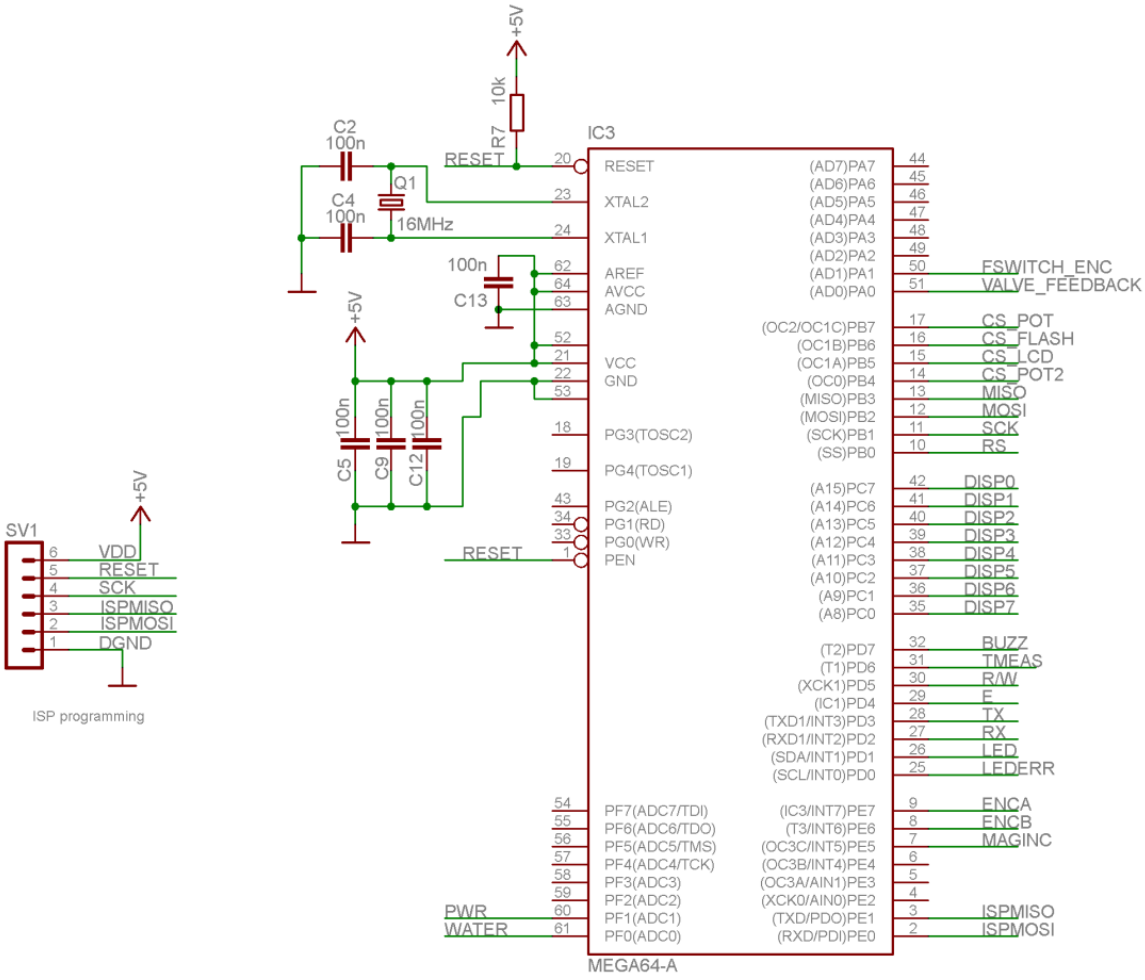

Fig. 5.9 ATMEGA64-A connection diagram

5.2.2 LCD display

A graphical display RG128646 is used [19]. Its resolution is 128x64 points. The supply pin VDD is connected to 5V power supply. The pin CS1 is used as “chip select”, when the state is high; the microcontroller communicates with the display. The RESET pin of LCD in not used, therefore it is kept in high state by pull-up resistor R4.

The pin A0 is used to distinguish between sending data or instructions. When the state is high, display data are sent; otherwise the instructions are sent. When the R/W pin is in high state, the data are written on the display; otherwise the data are read.

Pin E is the enable signal. With the rising edge of the enable signal, the data or instructions are sent from microcontroller are read. DB0-DB7 are pins for sending of 8-parallel data. The rest of the pins are connected through capacitors to the ground as it is recommended in [19].

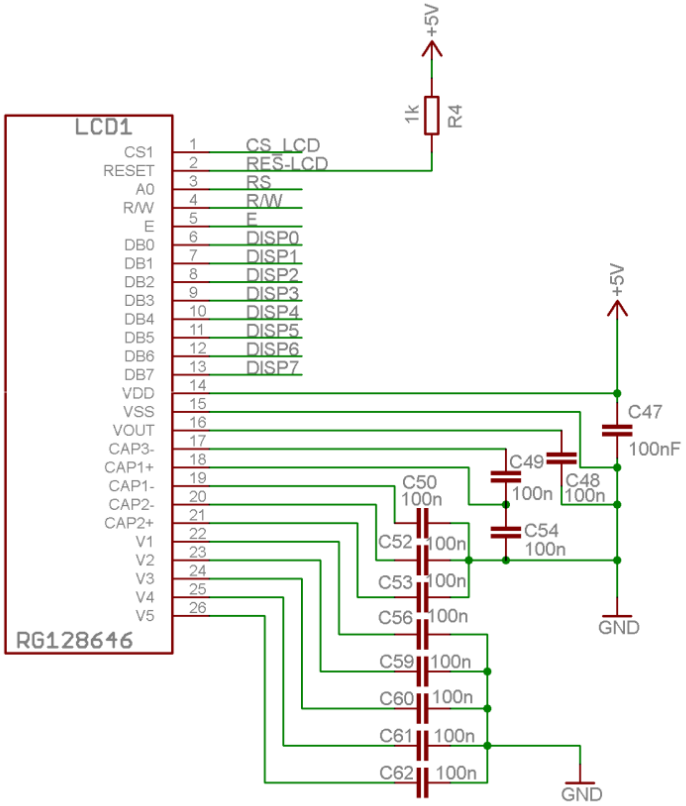

Fig. 5.10 LCD display connection diagram

5.2.3 Flash memory and temperature sensor

An additional 64kB serial flash memory FM25640 is used. It allows fast writing and reading of data with low power consumption [20]. The three signals are used to communicate with microcontroller via a serial line. The MOSI signal belongs to data sent from microcontroller to memory. The MISO signal is used to send data from memory to the microcontroller and SCK signal is the clock signal for serial line. Low state of the CS_FLASH signal chooses the peripheral device for communication. The flash memory provides an additional memory capacity to the microcontroller. If the internal memory of the microcontroller is sufficient, the flash memory is not assembled on the printed circuit board.

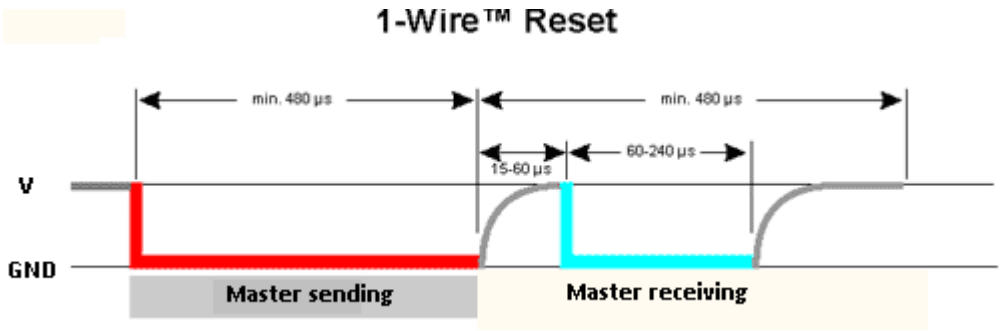

*Fig. 5.11 **1-wire** bus communication example*

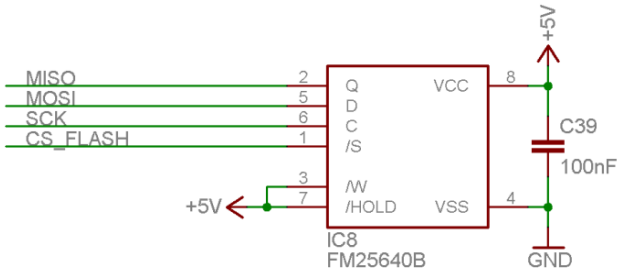

Fig. 5.12 Flash memory connection diagram

A temperature sensor is used to measure temperature inside the case. If the temperature rises too high, the microcontroller can shut down the device. Except this, the operational amplifier has also an internal overheating protection. These allow protecting the device to fail due to overheating.

As the digital thermometer the sensor DS18B20 manufactured by the Dallas semiconductors company is used [21]. It is connected to the microprocessor via a unique 1-wire interface. It only needs one wire for data and ground wire. It can be powered from the data line. However that feature is not used in the connection, which is shown on Fig. 5.13. The data wire is hold in high state by the pull-up resistor R14. The communication protocol description follows.

The communication begins with the master reset pulse. It means the data line is hold in low state for more than 480μs. Than the line is in high state and the master is "listening" (waiting for data). If there is an active device on the line, it puts the line into low state for 60-240 μs to report its presence. Next the master can start sending or receiving data. The data are sent in time slots with duration 60-120 μs. In one slot one bit of the data is sent. Between each slot there must be a 1 μs pause, when the line is in normal state. Then the algorithm of microcontroller program can be [22]:

1) RESET(Fig. 5.11)

- Put line into low state for 480 μs.
- Release line and wait 70 μs.
- Read line, when the state is 0, there is a device connected to the line. If the state is 1, there is not an active device.
- Wait 410 μs.

2) WRITE logical 1

- Put line into low state for 6 μs.
- Release line and wait 64 μs.

3) WRITE logical 0

- Put line into low state for 60 µs.
- Release line and wait 10 µs.

4) READ

- Put line into low state for 6 µs.
- Release line and wait 9 µs.
- Read the state of the line which is equal to the bit of the sent data.
- Wait 55 µs.

  This timing is recommended according to [22].

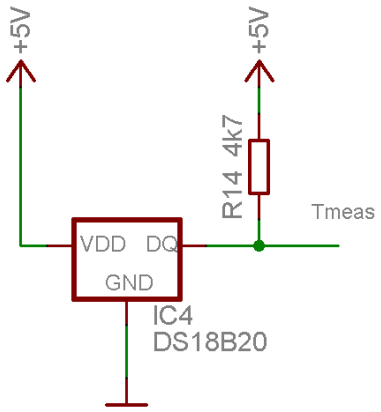

Fig. 5.13 DS18B20 thermosensor connection diagram

5.2.4 Magnetic encoder and buttons

Instead of keypad, the magnetic encoder and two buttons set is used. The magnetic encoder is used for its variability. It has a high angle resolution and it can simplify controlling of the device. The control is made by rotating and pressing the button.

One of the leading manufacturers of magnetic encoders is the Austria Microsystems company. In this project, the basic 10-bit model AS5040 [24] has been used.

Function of the encoder is based on the „Hall effect”. When there is a magnetic field applied to a conductor with electric current flowing through it, then a potential difference appears on the conductor in the direction perpendicular to both magnetic field orientation and current flow direction. This voltage is called “Hall voltage” and it is proportional to the value of current, magnetic flux density and thickness of the conductor and current density over the conductor. All the values except magnetic flux density can be considered as constants; therefore the measured voltage depends on the strength of the magnetic field which is proportional to the angle of rotation of the magnet.

So then if a transverse magnetized magnet rotates over the Hall probe, the amplified output is sine waveform. It can be assumed that in the range -45° to +45° is the conversion between the angle of rotation and voltage linear [25], Fig 4.13.

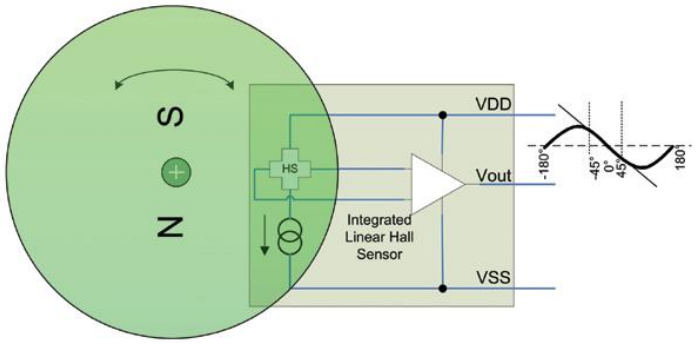

Fig. 5.14 Basic principle of a rotary magnetic encoder

The situation will change if there is a need to measure the angle of rotation in the range -360° to +360°. For that, an array of four Hall probes must be used. Then the phased shift signals are processed into a function, which linearly depends on the angle of rotation (green pattern on Fig. 5.15). Detailed information on processing of the signal can be found in [25]. The output data can be provided as PWM signal, serial data flow or quadrature.

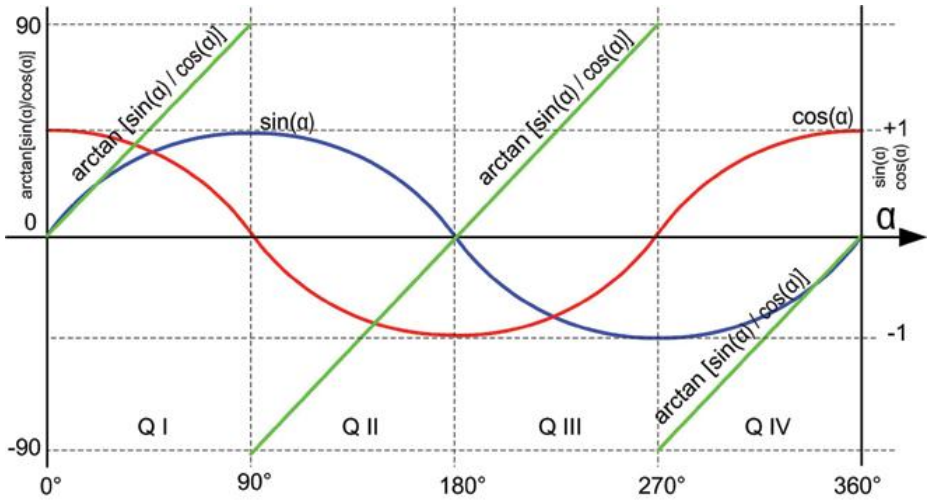

Fig. 5.15 Hall probes signal processing

The mechanical composition of the encoder consists of two parts. The first part is a round shaped button with magnet in the front panel and the second part is the integrated circuit mounted on the printed circuit board close enough to the magnet. The placement of the circuit on the PCB will be discussed later.

The connection diagram of the chip AS5040 can be seen on Fig. 5.17. The circuit is connected to 5V power supply, according to [24]. The pins 14 and 15 are connected through the electrolytic capacitor C3 to ground. There are three wires leading to the microcontroller. The MAGINC signal is set when the magnet gets closer to the chip. It signalizes increase of the magnetic field and therefore can be also used as a push

button for choice confirmation. The rotation of the button is used for menu listing or setting a value in steps.

The angle of rotation of the button is derived by the microcontroller from two signals signed ENCA and ENCB. These are rectangle signals that are phased shifted by 90°. The rising edge of the A signal causes interruption of the microcontroller and starts the interruption program for the magnetic encoder. After a short delay, the microcontroller reads the value of the signal B. If the value is 1, the value of a counter register is incremented. If the value of the B signal is 0, the value of the counter register is decremented. This interruption is activated with every rising edge of the A signal. The quadrature output signal is generated only when the angle is changing. The amount of generated squares is 256 per revolution. The width of the rectangle is 1µs (Fig. 5.16).

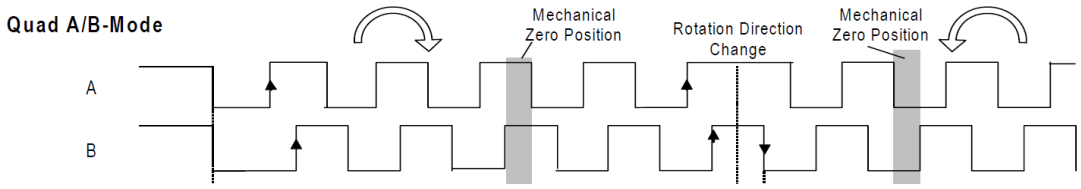

Fig. 5.16 Quadrature output signals

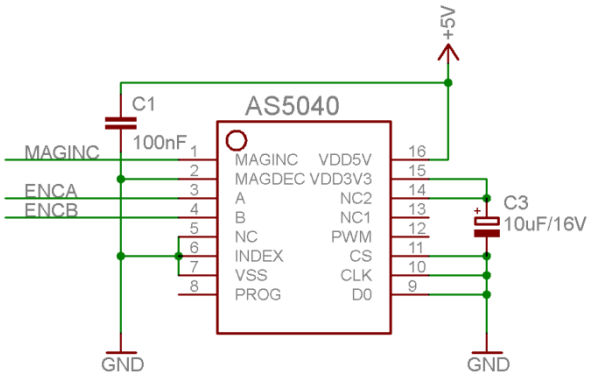

Fig. 5.17 AS5040 magnetic encoder connection diagram

In addition to the magnetic encoder, two micro switch buttons are used for quick access to the power and water flow adjustment.

5.2.5 FT232-RL

The USB interface is nowadays one of the common ways how to communicate with other devices. For example, there can be an intelligent tip holder, which can automatically recognize which tip is used and send the information to the main unit. Then the intensity is adjusted accordingly. Also the main unit can be connected to a computer and values such as setting of tip properties can be changed with the use of communication via USB port.

However, the used microcontroller does not include an USB transceiver. But it has an UART (universal asynchronous receiver/transmitter). The FT232-RL circuit is commonly used to convert the signals between the UART and USB interface.

As can be seen from Fig. 5.18, the FT232-RL is connected to 5V supply. The input signals TX and RX are data signals coming from the UART unit of the microcontroller. The USB+ and USB- are data signals of the USB interface. The USB also needs a power supply connection (wire +5V and DGND).

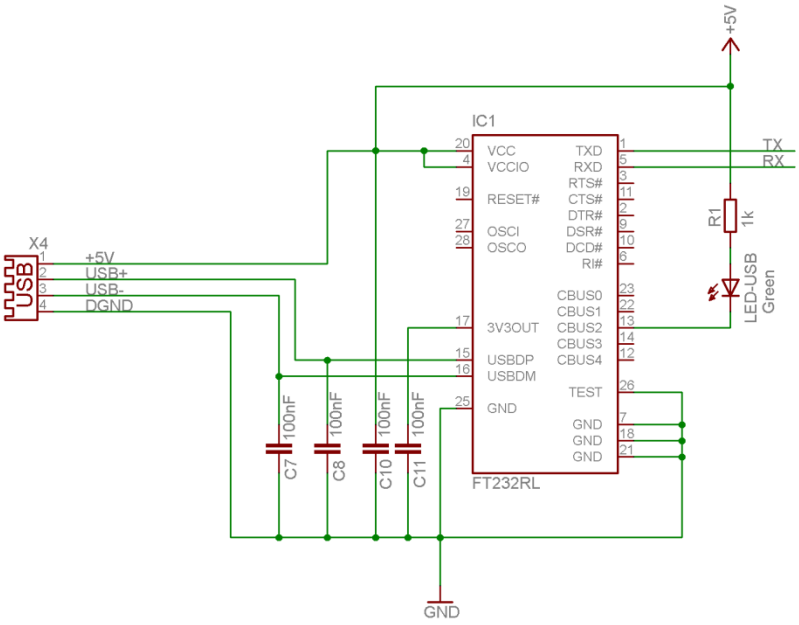

Fig. 5.18 FT232-RL UART/USB interface connection diagram

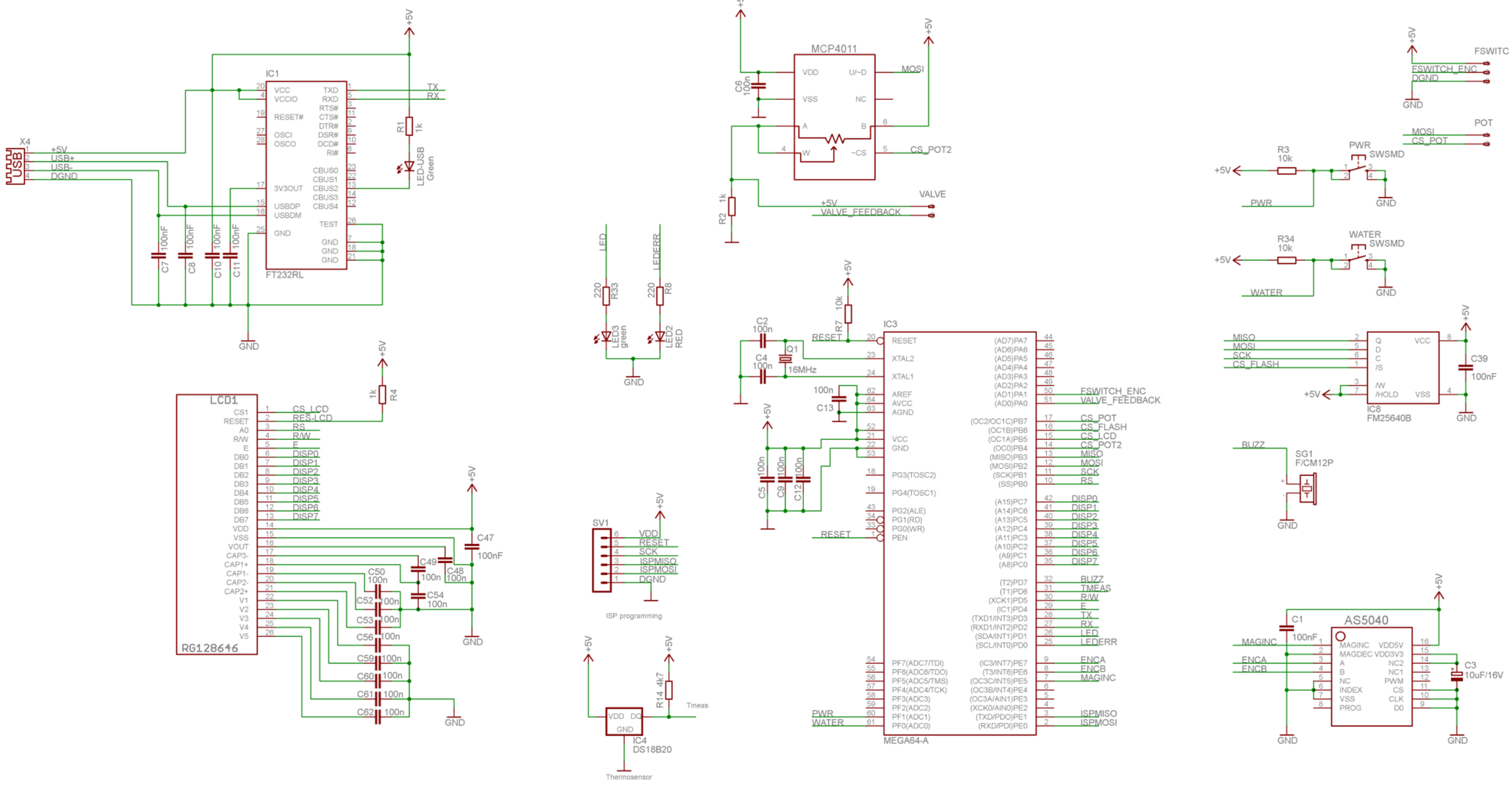

Fig. 5.19 Digital part connection diagram

5.3 Power supply circuits

5.3.1 Power balance sheet

When designing power supply, it is useful to create a power balance sheet (Table 3). It includes summary of the currents and voltages needed to feed the active components in circuitry. The values of supply voltage were mentioned above with the description of the connection diagram. The maximal values of supply current can be found in datasheets [12], [13] and [16]-[25].

Table 2 Power balance sheet

		18V	-18V	5V
Part name	Description	I[mA]	I[mA]	I[mA]
XR2206	Waveform generator	17,0	x	x
MCP4011	Digital potentiometer (valve control)	x	x	2,3
MCP4011	Digital potentiometer (amplitude setup)	x	x	2,3
OPA511	Operational amplifier	30,0	30,0	x
FT232RL	UART/USB interface	x	x	15,0
LCD RG128646	LCD graphical display	x	x	125,0
DS18B20	Thermosensor	x	x	1,5
AS5040	Magnetic encoder (front panel)	x	x	21,0
AS5040	Magnetic encoder (foot switch)	x	x	21,0
FM25640B	Flash memory	x	x	4,5
F/CM12P	Buzzer	x	x	13,0
HCPL0600	Optocoupler (MOSI)	x	x	5,0
TLP283	Optocoupler (CS)	x	x	5,0
HLMP-CM34	LED diode	25,0	x	x
Total		72,0	30,0	215,5

From the Table 3, it can be derived that there are three different power supplies needed. The last row of the table shows the required currents provided by the supplies.

Usually linear voltage regulators are used. Those are produced by various manufacturers. The main part of the identification is four-digit code. The first digit is 7. The second digit is 8, when the regulator provides positive output voltage. In the case of negative output voltage the second digit is 9. The other two digits show the output voltage value (for example 7805 provides 5V output). The letter L in the middle of the code states that output current is limited to 100 mA, otherwise it is 1A. The 5V voltage regulator will be connected to the output of the 18V regulator, so the required output current for the 18V regulator must be sum of required currents of both regulators.

So following voltage regulators can be used:

1) For power supply +18V/288 mA: integrated circuit 7818

2) For power supply -18V/30 mA: integrated circuit 79L18

3) For power supply +5V/216 mA: integrated circuit 7805

So there will be two positive and one negative voltage regulator. As the device will be connected to the electrical network with the alternating voltage value of 230V/50 Hz, the voltage must be transformed by a transformer, rectified and filtered before it comes to the input of the regulators.

The connection diagram of the power supply can be seen on Fig. 5.20.

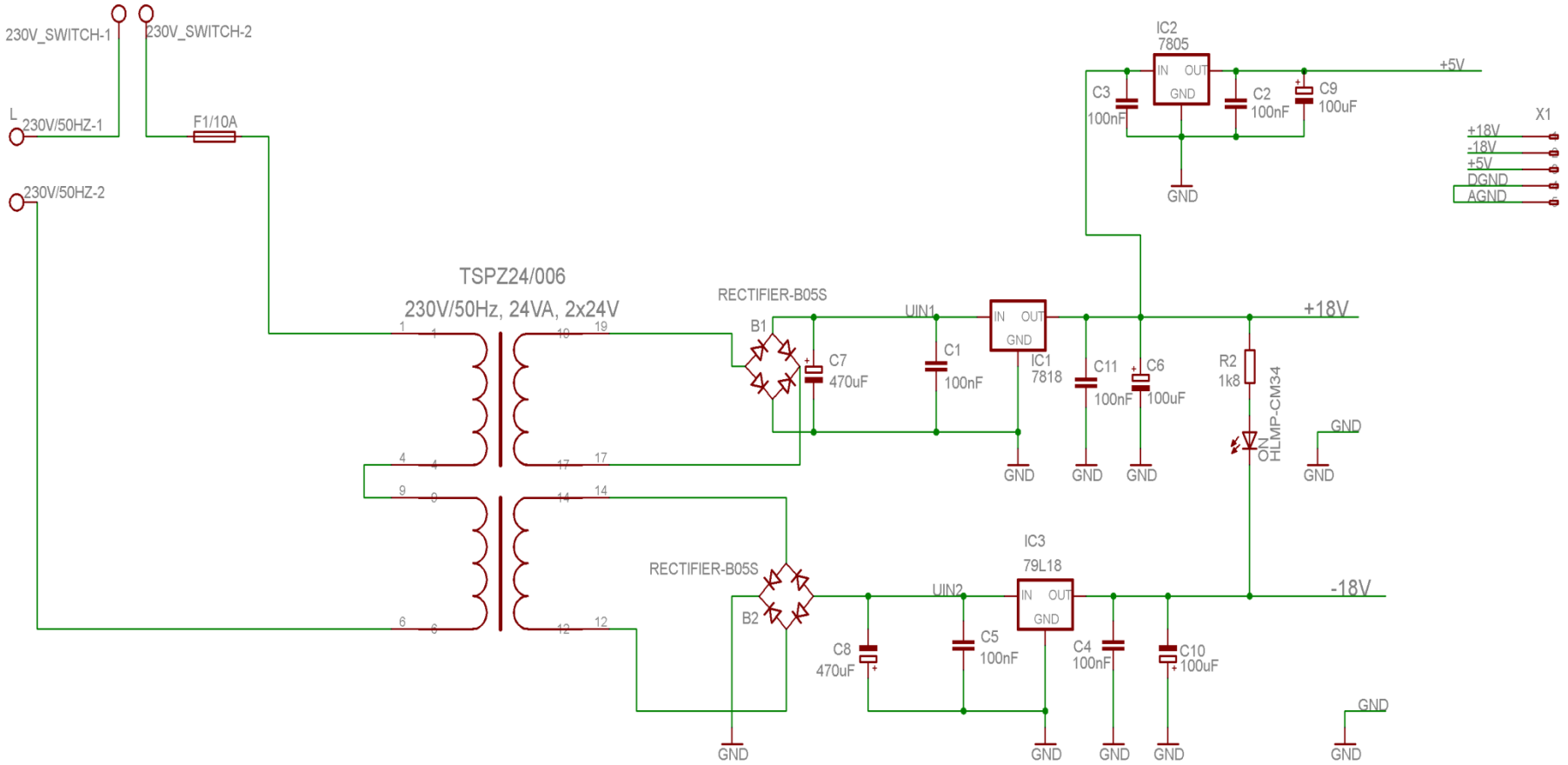

Fig. 5.20 Power supply connection diagram

5.3.2 Calculations of the power supply components

It is useful to start the calculations from the side of the regulators. It is known, that the effective value of the voltage on the output U_{18out} of the circuit 7818 is 18V. There is always a voltage dropout on a voltage regulator. The value of voltage dropout U_{18drop} for 7818 is 2V [29]. So the voltage UIN1 (Fig. 5.20) must be 2V higher, than the output voltage of the regulator [36]:

$$UIN1 = U_{18out} + U_{18drop} = 18 + 2 = 20V. \tag{5.22}$$

If we use a bridge rectifier, there is also a voltage dropout on rectifying diodes. All the time, the current flows through two silicone diodes with forward voltage U_d = 0,6V. The required transformer secondary winding voltage U_{trafo} can be calculated as [36]:

$$U_{trafo} = UIN1 + 2 \cdot U_d = 20 + 1{,}2 = 21{,}2V. \tag{5.23}$$

The calculations for the negative regulator 79L18 are identical to those made for 7818, just the connection to the secondary winding is opposite. So the transformer with two secondary windings and secondary voltage 24V is suitable.

It is important to compute the minimal transfer power for the transformer. It can be calculated from the basic formula for calculating of power [VA]:

$$P = U \cdot I\ . \tag{5.24}$$

The power for both windings is then is the sum of power in each winding:

$$\begin{aligned} P = P_1 + P_2 = U_{sec1} \cdot I_{sec1} + U_{sec2} \cdot I_{sec2} = \\ = 24 \cdot 0{,}288 + 24 \cdot 0{,}03 = 7{,}6\ VA. \end{aligned} \tag{5.25}$$

Once the values of secondary voltage and transfer power are known, a transformer can be chosen. A suitable transformer is TSPZ24/006 produced by the company EZK [32]. The primary winding is designed for electrical network voltage 230V/50Hz. It has two secondary windings with voltage 24V and the maximal transfer power is 24VA.

One more calculation should be done to prove the design. According to [37], the voltage of the electrical network can vary in the range $\pm$10%. It must be verified, that even in the limit case of 10% electrical network voltage drop and the device would work [36].

First we can calculate the transforming ratio as a ratio of secondary and primary voltage [-] [36]:

$$k = \frac{U_{sec}}{U_{prim}} = \frac{24}{230} = 0{,}104\ . \tag{5.26}$$

If we expect 10% decrease in electrical network voltage, then the value of primary voltage is:

$$U_{primlow} = 0{,}9 \cdot U_{prim} = 0{,}9 \cdot 230 = 207V. \quad (5.27)$$

The secondary voltage will be:

$$U_{seclow} = k \cdot U_{primlow} = 0{,}104 \cdot 207 = 21{,}6V. \quad (5.28)$$

This result proved that even if the electrical network voltage decrease, the secondary voltage will be still high enough for proper function of the device.

To rectify the alternating voltage, the bridge rectifier B05S is used. It is characterized by 1A output current [31], so it can be used for the power supply circuitry.

Last parts of the power supply circuitry are filter capacitors. The Fig. 5.21 shows rectified voltage on the output of the bridge rectifier. As this pattern consist half-sinewave pulses, it has to be filtered. The bold line shows the filtered signal. In the first quarter-period it follows the original signal. Once it reaches maximal value the capacitor is charged and the capacitor is uncharged. The uncharging is exponential and can be mathematically expressed as [36]:

$$U = U_{max} \cdot e^{-\frac{t}{R_Z \cdot C_n}}, \quad (5.29)$$

where U is the value of voltage in the time t, U_{max} value of the initial maximal voltage, R_Z load of the capacitor and C_n capacity of the capacitor.

With the use of the equation 5.29, the minimal capacity can be calculated as:

$$C_n = \frac{t}{R_z \cdot \ln\left(\frac{U_{max}}{U_{min}}\right)}, \quad (5.30)$$

where U_{max} is the maximal voltage on the output of the rectifier with value 32,8V. We require the voltage on the input of a regulator U_{min}=20V (equation 4.11).

The load resistance R_z can be calculated according to the Ohm's law as ratio of the output voltage and current provided by capacitor. For the voltage regulator 7818 is the load (for I_{7818}=288 mA, see Table 3):

$$R_Z = \frac{UIN1}{I_{7818}} = \frac{20}{0{,}288} = 69{,}5\Omega. \quad (5.31)$$

Finally the value of uncharging time [s] is needed, to calculate the minimal filter capacity. According to Fig. 5.21 [38], it can be computed as:

$$t = \frac{1}{4 \cdot T} + \frac{\arcsin\left(\frac{U_{min}}{U_{max}}\right)}{2 \cdot \pi} \cdot T, \quad (5.32)$$

where T is the value of the original electrical network voltage period (20ms) [37].

The uncharging time is:

$$t = \frac{1}{4 \cdot 0{,}02} + \frac{\arcsin\left(\frac{20}{32{,}8}\right)}{2 \cdot \pi} \cdot 0{,}02 = 7{,}087\text{ms}. \tag{5.33}$$

Next the minimal filter capacity for the voltage regulator 7818 is calculated (equation 4.20):

$$C_{n7818} = \frac{0{,}007087}{69{,}5 \cdot \ln\left(\frac{32{,}8}{20}\right)} = 206{,}2\ \mu F. \tag{5.34}$$

For the negative voltage regulator, the situation is exactly the same, only the value of the resistance is different, so we can calculate (I_{7918}=30 mA, see Table 3):

$$R_Z = \frac{UIN2}{I_{7918}} = \frac{20}{0{,}03} = 666{,}7\Omega \tag{5.35}$$

The minimal filter capacity is (equation 5.30):

$$C_{n7918} = \frac{0{,}007087}{666{,}7 \cdot \ln\left(\frac{32{,}8}{20}\right)} = 21{,}5\ \mu F. \tag{5.36}$$

Therefore the filter capacitor 470 µF/50V CE-470 [33] can be used in this application.

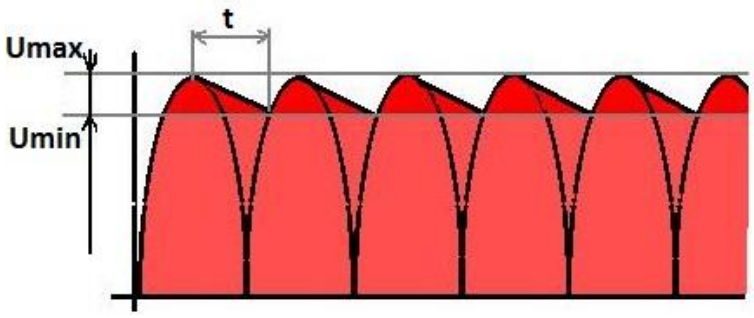

Fig. 5.21 Rectified voltage filtering

As it can be seen on Fig.5.20, there is a LED diode connected between the outputs of the +18V and -18V power supplies. The diode is on when both supplies work properly. The forward voltage U_d of the diode is 3,2V and forward current I_d is 20mA [34]. The voltage difference between the two supplies U_s is 36V. With these values, we can compute the resistance of the resistor R2 as:

$$R2 = \frac{U_s - U_d}{I_d} = \frac{36 - 3{,}2}{0{,}02} = 1640\Omega.. \tag{5.37}$$

So the chosen value of the resistor R2 is 1,8kΩ.

The primary winding of the transformer is connected to plug wire via an euro-connector. The input protected by a 10A fuse and can also include switch to completely turn off the device.

5.3.3 Piezoelectric valve

To control the flow of the water through the applicator, a piezoelectric valve is used. It is a suitable replacement of the classical electromagnetic valve. The advantages are low consumption, precision and speed. There are a few kinds of piezoelectric valves. As the requirement for the flow of water of the dental scaler is 20ml/min [10], the version for low flow control is used. It is called linear pinch valve. It is manufactured by the DTI Company [35].

The basic principle of work is very easy. It can be seen on Fig. 5.22 [35]. The fluid flows through inlet into compression tubing, which is pressed by a piston moved by a bidirectional piezo-motor. Then the flow depends on the position of the piston. The valve includes an internal feedback loop providing precise positioning. Furthermore there can be an external feedback loop connected (wire VALVE_FEEDBACK on Fig. 5.19). The valve is controlled by a DC voltage in the range 0-5V. The control voltage is provided by a voltage divider consisting of a 1kΩ resistor and digital potentiometer MCP4011, which was described earlier [35]. The supply voltage is in the range 5-12V. So the 5V power supply can be used.

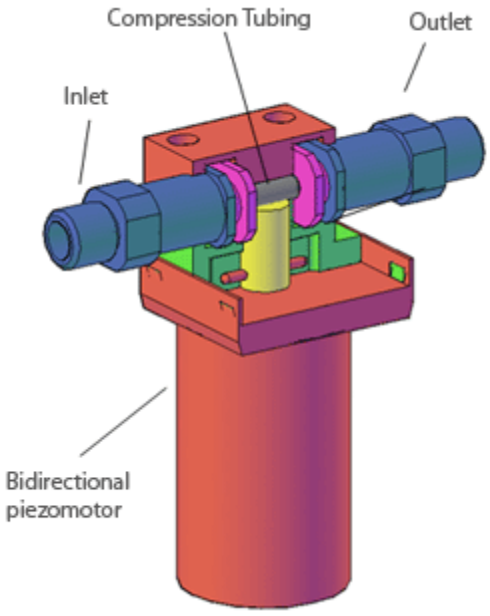

Fig. 5.22 Linear pinch valve

6. Manufacturing materials

Usually, when there are mixed analog and digital signals in the circuitry, there is an effort to divide the ground wires of analog and digital part and connect them as close to the power supply as possible. Also as there may be some changes necessary later in the process of testing, it is useful to design a printed circuit board for each functional unit.

Therefore there will be three PCB's. The first one is for the power supply; the second one for the digital control circuits; and finally the third one for the generator. Furthermore there will be the valve and foot switch as independent units.

The connection of PCB's can be seen on Fig. 6.1.

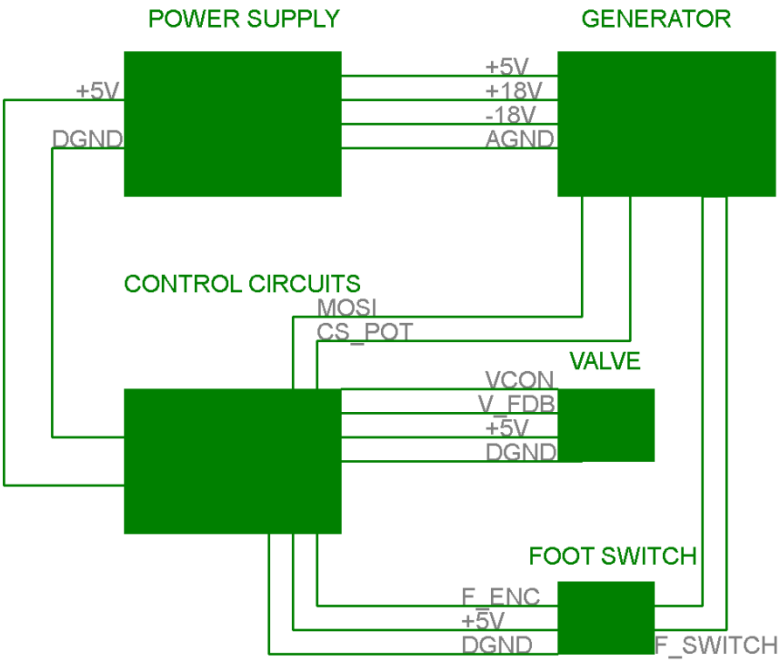

Fig. 6.1 PCB's connection diagram

6.1 Generator printed circuit board

The PCB of the generator part can be seen on Fig. 6.2. The ratio of the picture is 1:1. The dimensions are 100x60 mm. All the parts are located on the top side of the PCB (Fig. 6.3). The width of the routes is 0.6 mm, which is sufficient for currents up to 100 mA. There are holes in the corners of the board with diameter of 6 mm, which are used for mounting of the board to the case. The board will be located horizontal at the bottom of the case in front (Fig. 6.8).

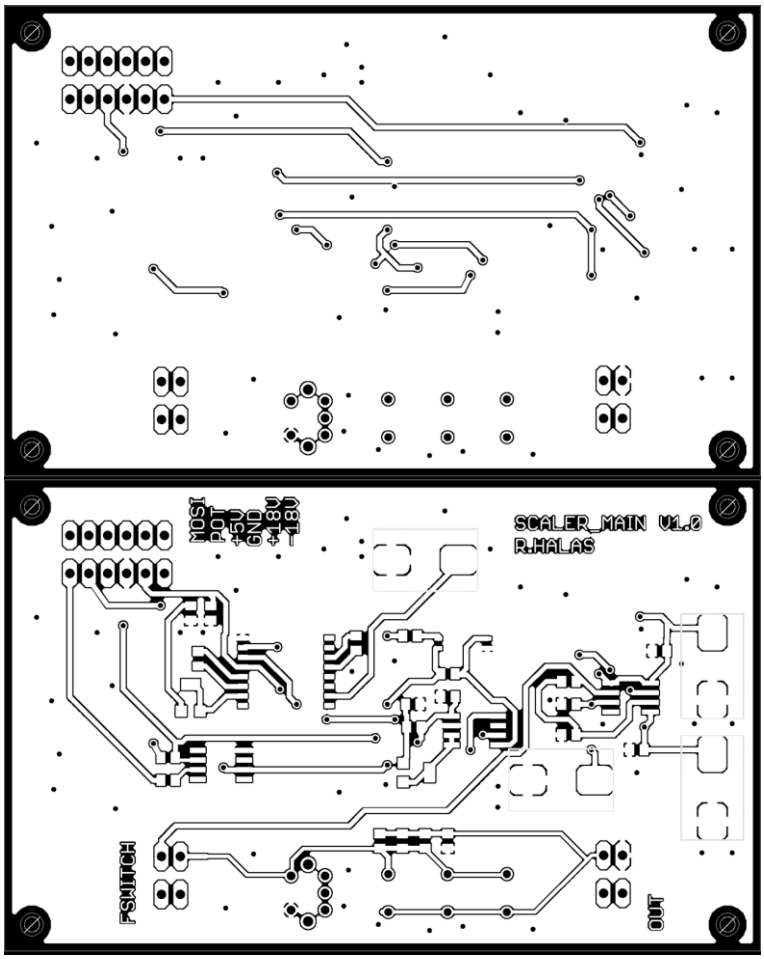

Fig. 6.2 Generator printed circuit board a) bottom side b) top side

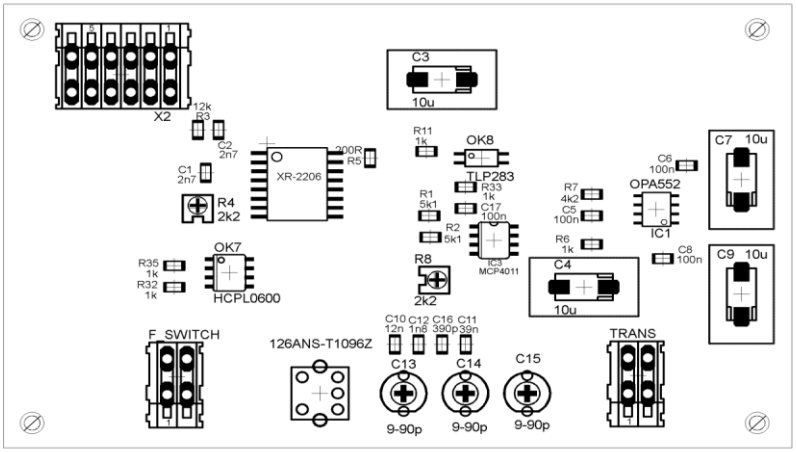

Fig. 6.3 Generator assembly diagram

6.2 Control circuits printed circuit board

The PCB of the control circuits can be seen on Fig. 6.5. It is has also two layers. The ratio of the picture is 1:1 and its real dimensions are 100x80 mm. As the current in this part is considerably lower and with respect to the size of the pads of parts, the 0,4 mm routes are used. The position of the board will be vertical in front of the device. There are four holes with 6mm diameter in the corners. On the assembly diagram (Fig. 6.5), it can be seen that on top side there are only parts which are used for front panel such as the magnetic encoder, two signaling LED diodes and two buttons. The rest of the parts are mounted on the bottom side. On the left side of the device, there will be the USB connector.

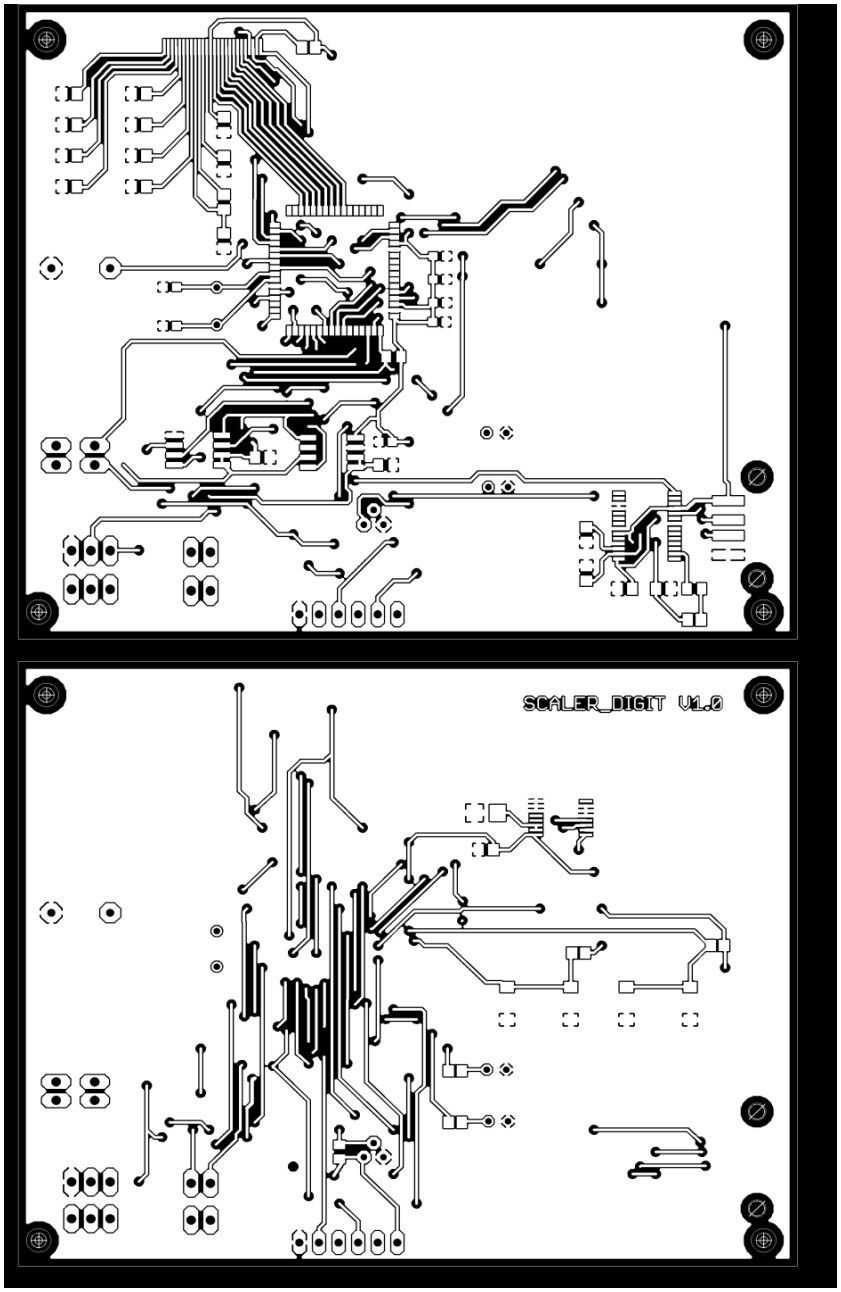

Fig. 6.4 Control circuits printed circuit board a) bottom side b) top side

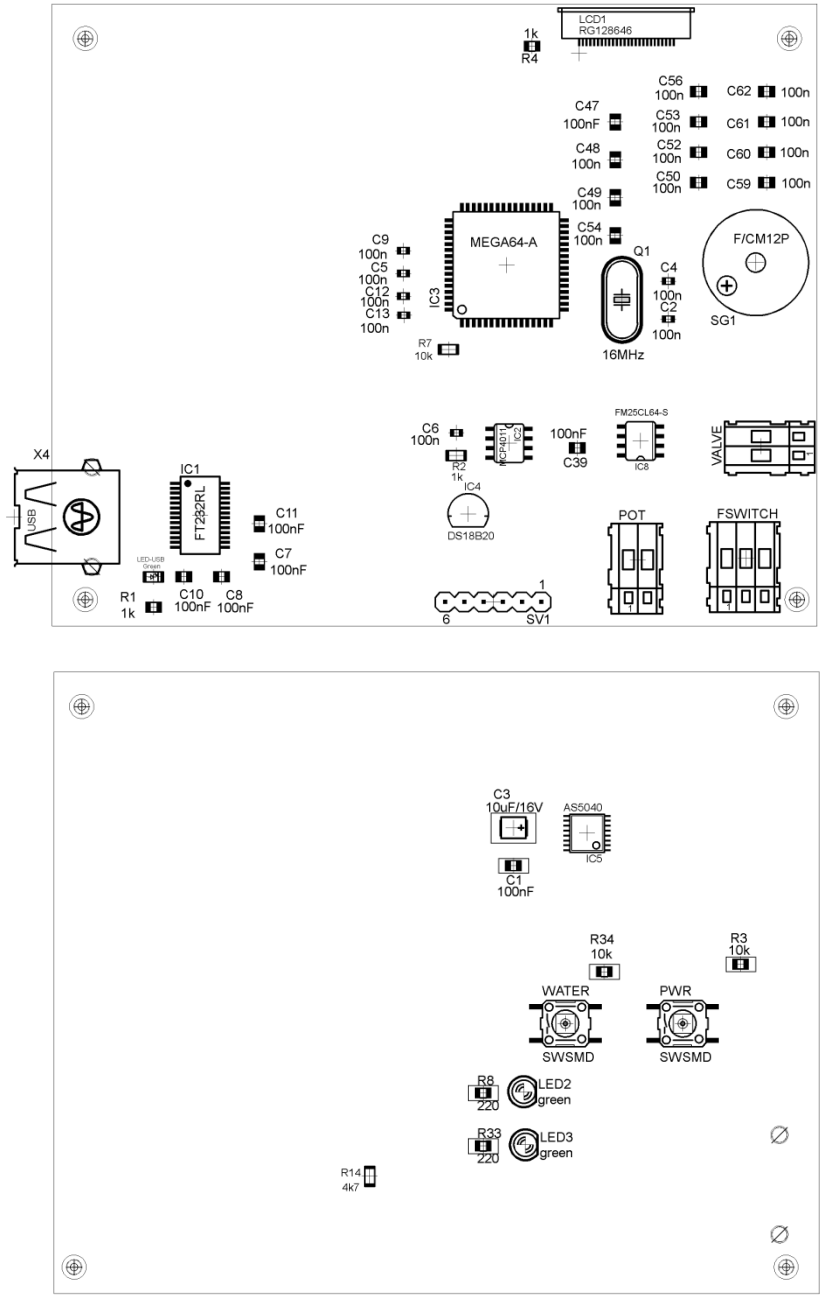

Fig. 6.5 Control circuits assembly diagram a) bottom side b) top side

6.3 Power supply printed circuit board

The last PCB belongs to the power supply. It can be seen on Fig. 6.6. As the circuitry is quite simple, the PCB has only one layer. The ratio of the picture is again 1:1 and its real dimensions are 100x100 mm. The current in this part is higher, so the routes width was designed as 1,2 mm. The PCB is placed horizontally at the bottom of the case in the rear part. The connectors 230V/50Hz and 230V_switch are connected by

wires to the euro-connector and switch on the rear wall of the case. There are four rectangle holes with the size of 6 mm for the transformer mounting

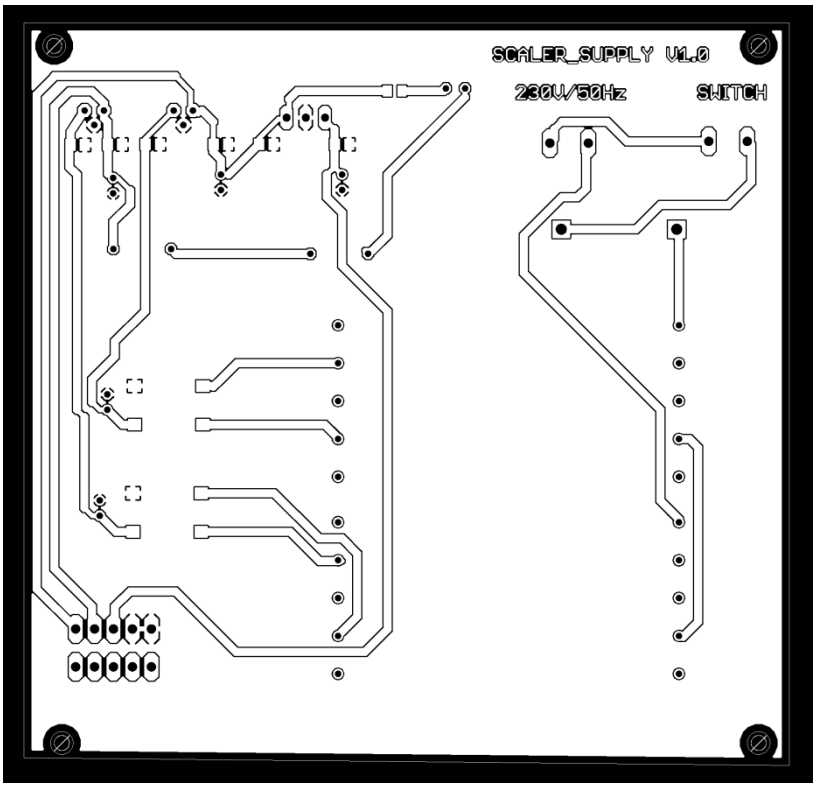

Fig. 6.6 Power supply printed circuit board

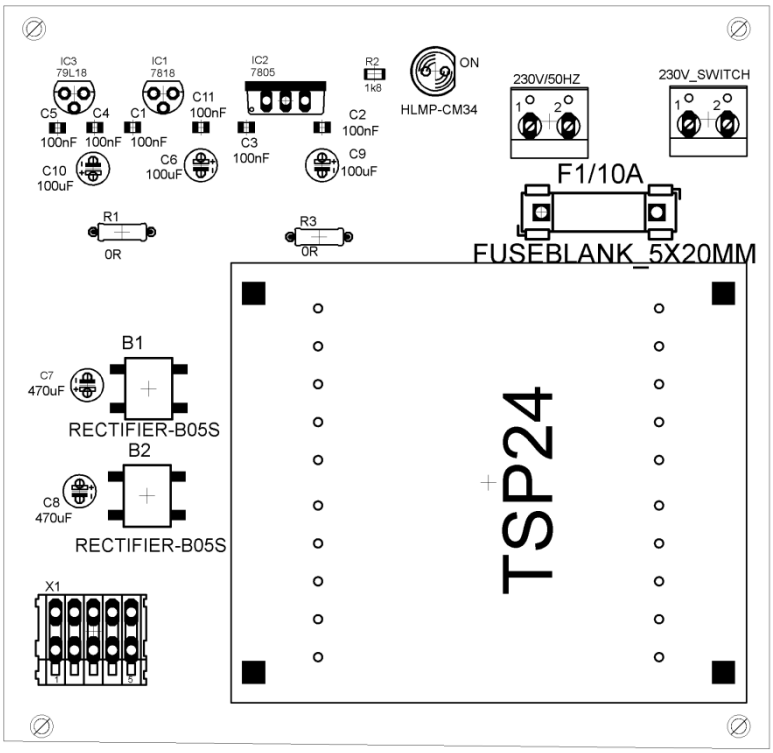

Fig. 6.7 Power supply assembly diagram

6.4 Power supply part list

Part	Value	Package	Description
230V/50HZ		W237-132	WAGO SREW CLAMP
230V_SWITCH		W237-132	WAGO SREW CLAMP
B1		B05S	BRIDGE RECTIFIER
B2		B05S	BRIDGE RECTIFIER
C1	100nF	C0805	CAPACITOR
C2	100nF	C0805	CAPACITOR
C3	100nF	C0805	CAPACITOR
C4	100nF	C0805	CAPACITOR
C5	100nF	C0805	CAPACITOR
C6	100uF	E2-4	POLARIZED CAPACITOR
C7	470uF	E2-4	POLARIZED CAPACITOR
C8	470uF	E2-4	POLARIZED CAPACITOR
C9	100uF	E2-4	POLARIZED CAPACITOR
C10	100uF	E2-4	POLARIZED CAPACITOR
C11	100nF	C0805	CAPACITOR
F1/10A	10A	FUSE_HOLDER	FUSE
IC1	LM7818	TO92	18V POSITIVE V. REGULATOR
IC2	LM7805	TO220V	5V POSITIVE V. REGULATOR
IC3	LM79L18	TO92	18V NEGATIVE VOLTAGE REGULATOR
ON	HLMP-CM34	LED5MM	LED
R2	1k8	0805	RESISTOR
T1	TSPZ24/006	TSPZ24/006	TRANSFORMER
X1		W233-105	WAGO SREW CLAMP

6.5 Digital control circuits part list

Part	Value	Package	Description
C1	100nF	C0805	CAPACITOR
C2	100n	C0603	CAPACITOR
C3	10uF/16V	CT3528	POLARIZED CAPACITOR
C4	100n	C0603	CAPACITOR
C5	100n	C0603	CAPACITOR
C6	100n	C0603	CAPACITOR
C7	100nF	C0805	CAPACITOR
C8	100nF	C0805	CAPACITOR
C9	100n	C0603	CAPACITOR
C10	100nF	C0805	CAPACITOR
C11	100nF	C0805	CAPACITOR
C12	100n	C0603	CAPACITOR
C13	100n	C0603	CAPACITOR

C39	100nF	C0805	CAPACITOR
C47	100nF	C0805	CAPACITOR
C48	100n	C0805	CAPACITOR
C49	100n	C0805	CAPACITOR
C50	100n	C0805	CAPACITOR
C52	100n	C0805	CAPACITOR
C53	100n	C0805	CAPACITOR
C54	100n	C0805	CAPACITOR
C56	100n	C0805	CAPACITOR
C59	100n	C0805	CAPACITOR
C60	100n	C0805	CAPACITOR
C61	100n	C0805	CAPACITOR
C62	100n	C0805	CAPACITOR
FSWITCH		233-103	WAGO SCREW CLAMP
IC1	FT232RL	SSOP28	UART/USB INTERFACE
IC2	MCP4011	SO-8	DIGITAL POTENTIOMETER
IC3	MEGA64-A	TQFP64	MICROCONTROLLER
IC4	DS18B20	TO92	THERMOSENSOR
IC8	FM25CL64	SO-8	FLASH MEMORY
LCD1	RG128646	CON26P	LCD DISPLAY
LED-USB	GREEN	LED0805	LED
LED2	GREEN	LED 3MM	LED
LED3	ORANGE	LED 3MM	LED
POT		233-102	WAGO SCREW CLAMP
PWR		SWTCHSMD	SMD SWITCH
Q1	16MHz	HC49U70	CRYSTAL
R1	1kΩ	R0805	RESISTOR
R2	1kΩ	R0805	RESISTOR
R3	10kΩ	R0805	RESISTOR
R4	1kΩ	R0805	RESISTOR
R7	10kΩ	R0805	RESISTOR
R8	220Ω	R0805	RESISTOR
R14	4,7kΩ	R0805	RESISTOR
R33	220Ω	R0805	RESISTOR
R34	10kΩ	R0805	RESISTOR
SG1		F/CM12P	BUZZER
SV1		MA06-1	PIN HEADER
AS5040		TSSOP16	MAGNETIC ENCODER
VALVE		233-102	WAGO SCREW CLAMP
WATER		SWTCHSMD	SMD SWITCH
X4		USB-A003	USB CONNECTOR

6.6 Generator circuits part list

Part	Value	Package	Description
126ANS-T1096Z	1-15 mH	71K	ADJUSTABLE COIL
C1	2n7	C0805	CAPACITOR
C2	2n7	C0805	CAPACITOR
C3	10u	085CS_1AW	POLARIZED CAPACITOR
C4	10u	085CS_1AW	POLARIZED CAPACITOR
C5	100n	C0805	CAPACITOR
C6	100n	C0805	CAPACITOR
C7	10u	085CS_1AW	POLARIZED CAPACITOR
C8	100n	C0805	CAPACITOR
C9	10u	085CS_1AW	POLARIZED CAPACITOR
C10	12n	C0805	CAPACITOR
C11	39n	C0805	CAPACITOR
C12	1n8	C0805	CAPACITOR
C13	9-90p	CTRIMTZ03	TRIMM CAPACITOR
C14	9-90p	CTRIMTZ03	TRIMM CAPACITOR
C15	9-90p	CTRIMTZ03	TRIMM CAPACITOR
C16	390p	C0805	CAPACITOR
C17	100n	C0805	CAPACITOR
F_SWITCH		233-102	WAGO SCREW CLAMP
IC1	OPA511	SO08	OPERATIONAL AMPLIFIER
IC2	XR-2206	XR-2206	WAVEFORM GENERATOR
IC3	MCP4011	SO-8	DIGITAL POTENTIOMETER
OK7	HCPL0600	SOIC08	OPTOCOUPLER
OK8	TLP283	MINI-FLAT	OPTOCOUPLER
R1	5,1kΩ	0805	RESISTOR
R2	5,1kΩ	0805	RESISTOR
R3	12kΩ	0805	RESISTOR
R4	2,2kΩ	RTRIM3304W	TRIMM RESISTOR
R5	200Ω	0805	RESISTOR
R6	1kΩ	0805	RESISTOR
R7	4,2kΩ	0805	RESISTOR
R8	2,2kΩ	TRIMM RESISTOR	TRIMM RESISTOR
R11	1kΩ	0805	RESISTOR
R32	1kΩ	0805	RESISTOR
R33	1kΩ	0805	RESISTOR
R35	1kΩ	0805	RESISTOR
TRANS		233-102	WAGO SCREW CLAMP
X2		233-106	WAGO SCREW CLAMP

7. Conclusion

In this project the ultrasonic dental scaler was designed. At the beginning, the theoretical background of dental calculus creation was described. The principles of the few methods used for the calculus removal were mentioned with focus on the ultrasonic method, which is the most common way of the treatment.

Based on the survey of function of some present manufactured devices, the functional and block diagram were built. First, the part of the applicator was designed. A sandwich transducer was used to excite ultrasonic wave with frequency of 27 kHz and tip maximum intensity 5 W/cm^2. The dimensions of the additional mass were calculated in accordance with the Langevin's equations. The material of the additional mass was chosen as titanium because of its good properties for ultrasound propagation.

The design of the applicator part was completed by calculation of the waveguide, which amplifies the ultrasonic wave and reduces the area of the working tool towards tip. Once the applicator was designed, the generator output power was calculated. The required output voltage of the generator was calculated as 11V.

Next, the circuits of generator (oscillator, amplifier) were created in order to deliver sufficient power to the transducer. As oscillator, the integrated circuit XR2206 was used to create sine-wave signal which is amplified by the high output current operational amplifier OPA552.

The output intensity, amount of water flowing towards the tip and some other variables are controlled by the digital unit. The main part of the unit is 8-bit microcontroller ATMega 64A. The user interface is created by the rotary magnetic encoder, set of two buttons and the graphical LCD display. The communication with other devices is possible via the USB port.

As the last part, the power supply unit was designed. This unit provides stable DC voltage of three values +18V,-18V, and +5V.

On the basis of the connection diagrams, the printed circuit board layouts were created for all free functional units. The design of the device is accompanied by diagram of connection and placement of the circuit boards in the case. The look of the case was also proposed.

All the previously mentioned steps in addition to the part lists, PCB diagrams and technical drawings create a set of materials that is necessary for the construction of the dental scaler.

For the next development of the device the following steps are proposed:

- Manufacture the printed circuit boards, connect and test them
- Create the program for the microcontroller

- Design the foot switch
- Assembly the device in accordance to materials proposed in this thesis

The combination of the system design carried out in this project and the above mentioned steps will lead to the fully functional device which will be ready for testing and later for the market approval.

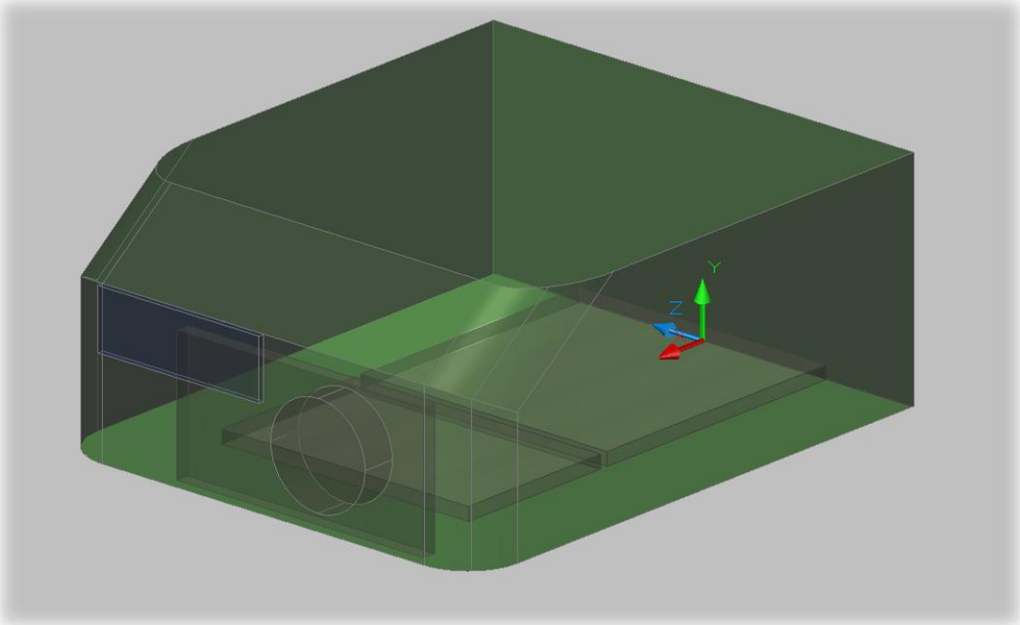

Fig. 6.8 Device design

List of pictures

Literature

[1] Cochran, L.D.Plaque and Calculus Removal: Considerations for the Professional. Quintessence Publishing Company. 1994. 99 p. ISBN-13: 9780867152852

[2] Calculus or Tooth Tartar Removal Procedure [online]. 2008. Dental Health Magazine. Available on WWW: <http://worldental.org/gums/calculus-or-tooth-tartar-removal-procedure/>

[3] Rozman, J. Ultrazvuková technika v lékařství. Brno: Ediční středisko VUT Brno, 1980, 264 p. ISBN 55-571-80

[4] Taraba, O; Vybrané stati z fyzikální akustiky I., Ultrazvuk, Praha: ČVUT, 1975, 427 p., ISBN 4- 690137

[5] *Scaling [online]. 2010. Amdent AB [cit. 2010-03-24]* Available on WWW: <http://www.amdent.se/index.php?action=expand&page=00340>.

[6] *Ultrasonic piezo scalers [online]. 2010. Amdent AB [cit. 2010-03-24]* Available on WWW: < http://www.amdent.se/index.php?action=expand&page=00047>.

[7] *Single Crystal Piezo [online]. 2010. Morgan Technical Ceramics [cit. 2010-03-24]* Available on: <http://www.morganelectroceramics.com/materials/piezoelectric/single-crystal-piezo/>.

[8] *Piezoelectric Standard Rings [online]. 2010. Morgan Technical Ceramics [cit. 2010-03-24]* Available on WWW: <http://www.morganelectroceramics.com/products/piezoelectric/piezoelectric-standard-rings/>.

[9] *Piezoelectricity. Technical Publication TP-235 [online]. 2008. Morgan Technical Ceramics [cit. 2010-03-24]* Available on WWW: < http://www.morganelectroceramics.com/resources/technical-publications/>.

[10] How to use your Amdent. Amdent AB. 9770151. Revision A 1999

[11] *Piezo Ceramic Tutorials [online]. 2008. Morgan Technical Ceramics [cit. 2010-03-24].* Available on: <http://www.morganelectroceramics.com/resources/piezo-ceramic-tutorials/>.

[12] Exar Corporation. XR-2206 datasheet.1997. 16 p. Available on WWW: <http://www.datasheetcatalog.com/datasheets_pdf/X/R/2/2/XR2206.shtml>

[13] Microchip Technology Incorporated. MCP4011 datasheet.2006. 60 p. Available on WWW: < http://www.alldatasheet.com/datasheet-pdf/pdf/197234/MICROCHIP/MCP4011.html >

[14] Kameníček, R. *Ultrazvukový indikátor toku krve.* (Diploma thesis) Brno : VUT, 2009. 72 p.

[15] Hanus, S., Svačina, J. Vysokofrekvenční a mikrovlnná technika. UREL VUT, BRNO 2005. 210 p. ISBN 80-214-2222-X

[16] HUBER+SUHNER AG. 179 B/U coaxial cable datasheet.2004. 2 p. Available on WWW: < http://www.repic.co.jp/contents/products/huber/seihin/rf/pdf/rg179bu.pdf>

[17] Texas Instruments. OPA552 datasheet. 2003. 23 p. Available on WWW: < http://www.datasheetcatalog.com/datasheets_pdf/O/P/A/5/OPA552.shtml >

[18] Atmel Corporation. ATMEGA64A datasheet. 2009. 21 p. Available on WWW: <http://www.alldatasheet.com/datasheetpdf/pdf/197234/MICROCHIP/MCP4011.html >

[19] Apex Corporation. RG128646 datasheet.2006. 12 p. Available on WWW: < http://www.geniusnet.sk/om3bc/datasheets/RG128646-3YFHDYB.pdf>

[20] Ramtron International Corporation. FM25640 datasheet. 2003. 14 p. Available on WWW: < http://www.datasheetcatalog.com/datasheets_pdf/F/M/2/5/FM25640.shtml>

[21] Dallas Semiconductor. DS18B20 datasheet. 2005. 27 p. Available on WWW: < http://www.maxim-ic.com/datasheet/index.mvp/id/2812>

[22] Teploměr s čidlem DS18B20 . *2008. [cit. 2011-03-24]* Available on WWW: <http://hw.cz/teorie-praxe/konstrukce/art2277-teplomer-s-cidlem-dallas-ds18b20.html>

[23] *Sběrnice 1-wire [online]. 2004. [cit. 2011-03-24]* Available on WWW: < http://hw.cz/rozhrani/art1215-sbernice-1-wire.html>

[24] Austriamicrosystems. AS5040 datasheet. 2006. 28 p. Available on WWW: < http://www.austriamicrosystems.com/eng/Products/Magnetic-Encoders/Rotary-Encoders/AS5040/AS5040-Downloads/AS5040-Downloads>

[25] *Magnetic Encoders [online]. 2010.* Available on WWW: < http://www.austriamicrosystems.com/eng/austriamicrosystems

magnetic encoders products - linear encoders, easypoint joystick encoder, rotary encoders.mht>.

[26] Digisound. F/CM12P datasheet. 1999. 1 p. Available on WWW: < https://www.distrelec.hu/ishop/Datasheets/jp560671_d_e.pdf*buzzer*>

[27] Future Technology Devices Ltd.. FT232-RL datasheet. 2010. 43 p. Available on WWW: <http://www.ftdichip.com/Support/Documents/DataSheets/IC/DS_FT232R.pdf>

[28] Fairchild Semiconductors. LM7805 datasheet. 2001. 28 p. Available on WWW: <http://pdf1.alldatasheet.com/datasheetpdf/view/82833/FAIRCHILD/LM7805.html>

[29] Fairchild Semiconductors. LM7818 datasheet. 2001. 24 p. Available on WWW: <http://pdf1.alldatasheet.com/datasheetpdf/view/8833/FAIRCHILD/LM78L18.html>

[30] Fairchild Semiconductors. LM79L18 datasheet. 2001. 22 p. Available on WWW: < http://pdf1.alldatasheet.com/datasheet-pdf/view/82833/FAIRCHILD/LM78L18.html>

[31] Comchip 2003. B05S rectifier datasheet. 2004. 2 p. Available on WWW: < http://www.datasheetcatalog.com/datasheets_pdf/B/0/5/S/B05S.shtml>

[32] EZK. 2003. B05S rectifier datasheet. 2004. 1 p. Available on WWW: < *http://www.ezk.cz/trafa_INDEL_str2.pdf* >

[33] TME Czech Republic. CE-470/25 capacitor datasheet.1 p. Available on WWW: <*http://www.ezk.cz/trafa_INDEL_str2.pdf*>*http://www.tme.eu/html/CZ/axialni-elektrolyticke-kondenzatory/ramka_270_CZ_pelny.html*>

[34] Avago Technologies. HLMP-CM34 LED diode datasheet. 2009. 10 p.Available on WWW: < http://www.avagotech.com/docs/AV02-0678EN>

[35] *Piezoelectric linear pinch valve [online]. 2010.* Available on WWW: < http://www.dti-piezotech.com/Docs/Linear_Pinch_Valve-4_13_10.pdf>

[36] Notes from the course MABD, lecturer: *Chmelař, M. VUT Brno. [cit. 2010-02-19]*

[37] *Návod na použití elektřiny pro domácnosti [online]. 2011. [cit. 2010-05-23]* Available on WWW:< *http://www.eon.cz/cs/info/guide.shtml*>

[38] Usměrňovače III - Výpočet filtrač. kondenzátoru *[online]. 2009. [cit. 2010-05-23]* Available on WWW:<*http://www.volta.estranky.cz/clanky/zdroje_-stabilizatory_-usmernovace/usmernovaceIII.html* >

Seznam použitých zkratek a symbolů

α	[-]	Koeficient útlumu
C		Značení kondenzátoru
C	[F]	Kapacita
C0	[F]	Statická kapacita měniče
d	[m]	Tloušťka
d_m	[m]	Tloušťka měniče
D	[m]	Průměr
ε_0	$\left[\frac{F}{m}\right]$	Permitivita vakua
ε_r	[-]	Relativní permitivita
η	[-]	Účinnost
f	[Hz]	Frekvence
GND		Zem
I	$\left[\frac{W}{m^2}\right]$	Intenzita
I	[A]	Elektrický proud
IC		Integrovaný obvod
I_i	$\left[\frac{W}{m^2}\right]$	Intenzita přímé vlny
I_r	$\left[\frac{W}{m^2}\right]$	Intenzita odražené vlny
k	[-]	Koeficient vazby
K	[-]	Koeficient zesílení vlnovodu
L	[H]	Indukčnost
L		Značení cívky
l	[m]	Délka

λ	[m]	Vlnová délka
N	$[Hz \cdot m]$	Frekvenční konstanta
P	[VA]	Elektrický výkon
PCB		Deska plošného spoje
PWM		Pulsně šířková modulace
R		Značení rezistoru
R	[Ω]	Elektrický odpor
r	[-]	Koeficient reflexe
ρ	$\left[\frac{kg}{m^3}\right]$	Hustota
S	[m^2]	Obsah
t	[s]	Čas
U	[V]	Elektrické napětí
U_{ef}	[V]	Efektivní hodnota el. napětí
U_{max}	[V]	Amplituda el. napětí
U_{in}	[V]	Vstupní napětí
U_{out}	[V]	Výstupní napětí
v	$\left[\frac{\mathrm{m}}{\mathrm{s}}\right]$	Rychlost šíření ultrazvuku
ω	$\left[\frac{rad}{m}\right]$	Úhlová rychlost
x	[m]	Vzdálenost
Y	$\left[\frac{N}{m^2}\right]$	Youngův modul pružnosti
Z	$\left[\frac{Pa \cdot s}{m^{-1}}\right]$	Akustická impedance

List of abbreviations and symbols

α	[-]	Attenuation coeffiecient
C		Symbol for capacitor
C	[F]	Capacity
C0	[F]	Static capacity of a transducer
d	[m]	Width
d_m	[m]	Width of transducer
D	[m]	Diameter
ε_0	$\left[\frac{F}{m}\right]$	Permitivity of the vacuum
ε_r	[-]	Relative permitivity
η	[-]	Efficiency
f	[Hz]	Frequency
GND		Ground
I	$\left[\frac{W}{m^2}\right]$	Intensity
I	[A]	Electric current
IC		Integrated circuit
I_i	$\left[\frac{W}{m^2}\right]$	Direct wave intensity
I_r	$\left[\frac{W}{m^2}\right]$	Reflected wave intensity
k	[-]	Coupling coefficient
K	[-]	Amflification coefficient
L	[H]	Inductance
L		Symbol for electric coil

l	[m]	Length
λ	[m]	Wavelength
N	$[Hz \cdot m]$	Frequency constant
P	[VA]	Electric power
PCB		Printed circuit board
PWM		Pulse-width modulation
R		Symbol for resistor
R	[Ω]	Electric resistance
r	[-]	Reflection coefficient
ρ	$\left[\frac{kg}{m^3}\right]$	Density
S	[m^2]	Area
t	[s]	Time
U	[V]	Electric voltage
U_{ef}	[V]	Root mean square voltage
U_{max}	[V]	Maximum voltage
U_{in}	[V]	Input voltage
U_{out}	[V]	Output voltage
v	$\left[\frac{\mathrm{m}}{\mathrm{s}}\right]$	Speed of ultrasonic waves propagation
ω	$\left[\frac{rad}{m}\right]$	Angular velocity
x	[m]	Distance
Y	$\left[\frac{N}{m^2}\right]$	Young module of elasticity
Z	$\left[\frac{Pa \cdot s}{m^{-1}}\right]$	Acoustic impedance

Seznam příloh

Příloha č.1 Výkres aplikátoru
Příloha č.2 Celkové schéma zapojení

List of appendices

Appendix No.1 Applicator drawing
Appendix No.2 Full connection diagram

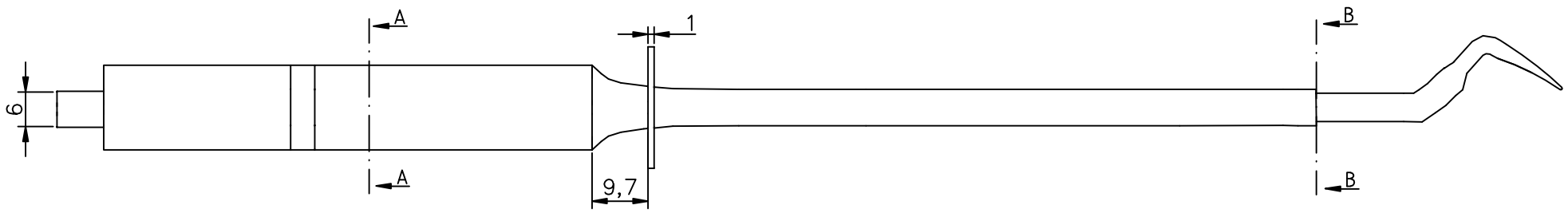

A-A(2:1)

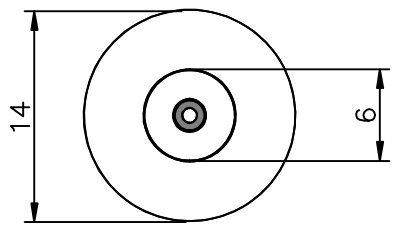

B-B(2:1)

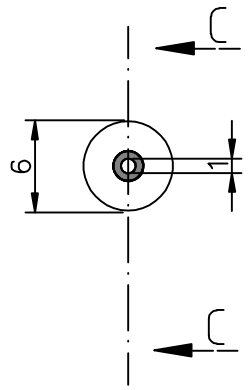

C-C(1:1)

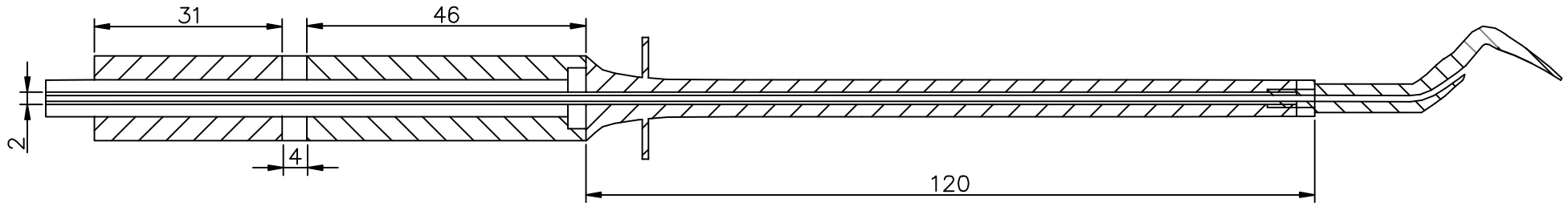

VUT FEKT UBMI	AUTHOR: ROSTISLAV HALAS	NAME: APLICATOR	RATIO: 1:1
	DATE: 10.6.2011	DRAWING NO.: 2.0	PAGE: 1/1

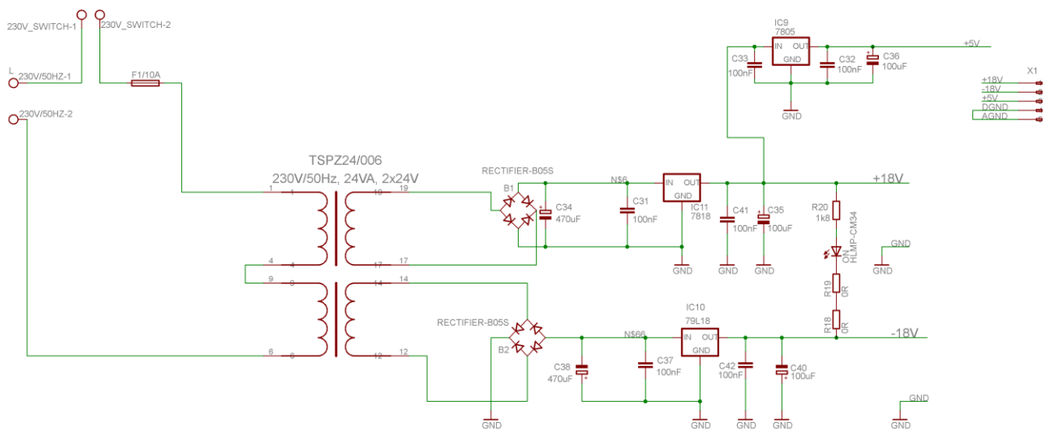
230V_SWITCH-1
230V_SWITCH-2
L
230V/50HZ-1
230V/50HZ-2
F1/10A
TSPZ24/006
230V/50Hz, 24VA, 2x24V
RECTIFIER-B05S
B1
C34 470uF
C31 100nF
IC11 7818
C41 100nF
C35 100uF
R20 1kB
+18V
GND
RECTIFIER-B05S
B2
C38 470uF
C37 100nF
IC10 79L18
C42 100nF
C40 100uF
R19 0R
R18 0R
-18V
IC9 7805
C33 100nF
C32 100nF
C36 100uF
+5V
X1
+18V
-18V
+5V
DGND
AGND

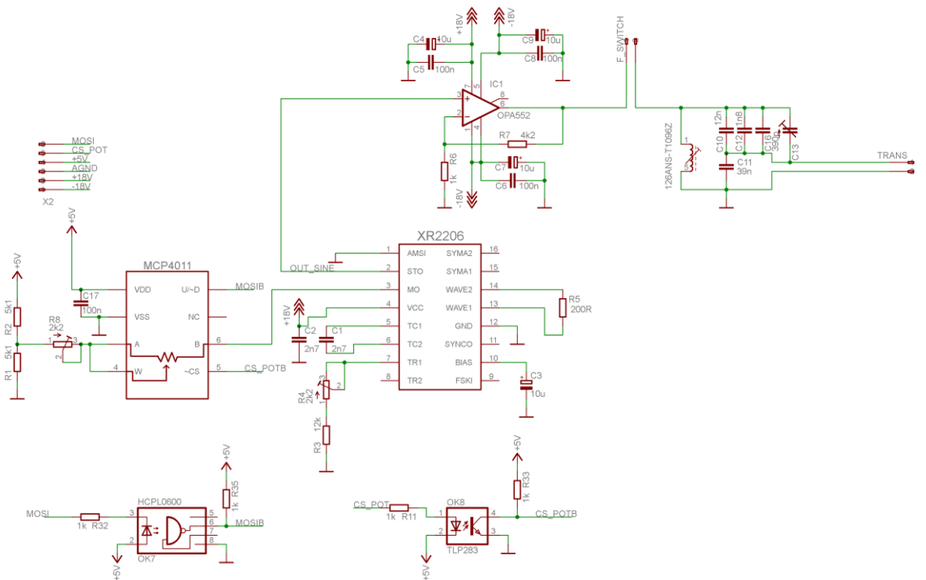
MOSI
CS_POT
+5V
AGND
+18V
-18V
X2
MCP4011
VDD
U/~D
VSS
NC
A
B
W
~CS
MOSIB
CS_POTB
C17 100n
R8 2k2
R2 5k1
R1 5k1
OUT_SINE
XR2206
AMSI
STO
MO
VCC
TC1
TC2
TR1
TR2
SYMA2
SYMA1
WAVE2
WAVE1
GND
SYNCO
BIAS
FSKI
C2 2n7
C1 2n7
R4 2k2
R3 12k
R5 200R
C3 10u
C4 10u
C8 100n
C9 10u
C5 100n
IC1
OPA552
R7 4k2
R6 1k
C7 10u
C6 100n
F_SWITCH
L1 126ANS-T109RZ
C10 2n
C12 n8
C14 390p
C13
C11 39n
TRANS
HCPL0600
OK7
R32 1k
R25 1k
OK8
TLP283
R11 1k
R33 1k

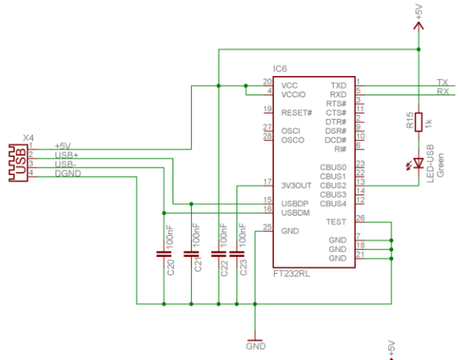
IC6
FT232RL
X4
+5V
USB+
USB-
DGND
TXD
RXD
RTS#
CTS#
DTR#
DSR#
DCD#
RI#
CBUS0
CBUS1
CBUS2
CBUS3
CBUS4
TEST
3V3OUT
USBDP
USBDM
GND
TX
RX
R15 1k
LED-USB Green
C20 100nF
C24 100nF
C22 100nF
C23 100nF

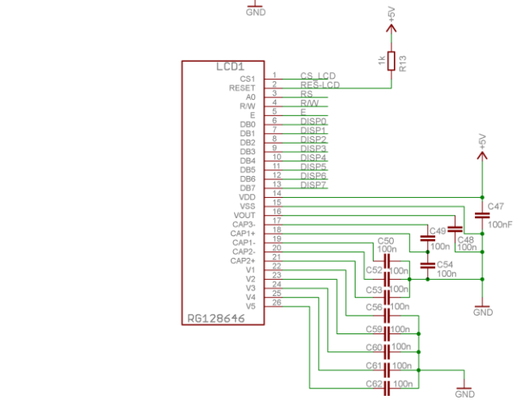
LCD1
RG128646
CS_LCD
RES_LCD
RS
R/W
E
DISP0
DISP1
DISP2
DISP3
DISP4
DISP5
DISP6
DISP7
R13 1k
C47 100nF
C49 100n
C48 100n
C54 100n
C50 100n
C52 100n
C53 100n
C56 100n
C59 100n
C60 100n
C61 100n
C62 100n

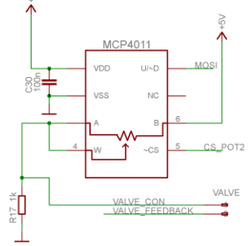
MCP4011
VDD
U/~D
VSS
NC
A
B
W
~CS
MOSI
CS_POT2
C30 100n
R_F 1k
VALVE
VALVE_CON
VALVE_FEEDBACK

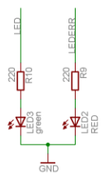
LED
LEDERR
220 R10
220 R9
LED3 green
LED2 RED
GND

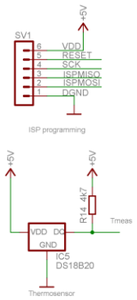
SV1
VDD
RESET
SCK
ISPMISO
ISPMOSI
DGND
ISP programming
+5V
R14 4k7
VDD
DQ
GND
IC5
DS18B20
Tmeas
Thermosensor

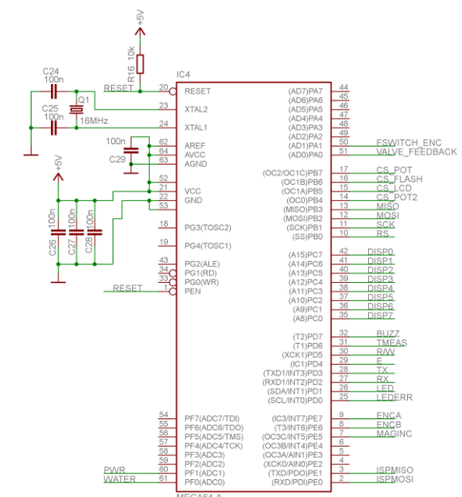
C24 100n
C25 100n
Q1
16MHz
C29 100n
C26 100n
C22 100n
C28 100n
R16 10k
RESET
IC4
MEGA64-A
XTAL2
XTAL1
AREF
AVCC
AGND
VCC
GND
PG3(TOSC2)
PG4(TOSC1)
PG2(ALE)
PG1(RD)
PG0(WR)
PEN
PWR
WATER
FSWITCH_ENC
VALVE_FEEDBACK
CS_POT
CS_FLASH
CS_LCD
CS_POT2
MISO
MOSI
SCK
RS
DISP0
DISP1
DISP2
DISP3
DISP4
DISP5
DISP6
DISP7
BUZZ
TMEAS
R/W
E
TX
RX
LED
LEDERR
ENCA
ENCB
MAGINC
ISPMISO
ISPMOSI

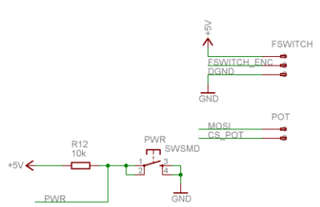
FSWITCH
FSWITCH_ENC
DGND
GND
POT
MOSI
CS_POT
R12 10k
PWR
SWSMD
PWR
GND
R34 10k
WATER
SWSMD
WATER
GND

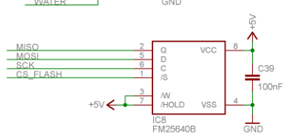
MISO
MOSI
SCK
CS_FLASH
Q
D
C
/S
/W
/HOLD
VCC
VSS
IC8
FM25640B
C39 100nF
+5V
GND

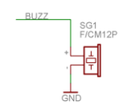
BUZZ
SG1
F/CM12P
GND

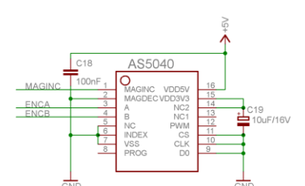
C18 100nF
AS5040
MAGINC
MAGDEC
A
B
NC
INDEX
VSS
PROG
VDD5V
VDD3V3
NC2
NC1
PWM
CS
CLK
DO
C19 10uF/16V
+5V
GND